Soil Dynamics and Its Application to Foundation Engineering

Dynamique du Sol et son Application aux Travaux de Fondations

Chairman/Président: H. B. Seed (U. S. A.)
General Reporter/Rapporteur-Général: Y. Yoshimi (Japan)
Co-Reporters/Co-Rapporteurs: V. A. Ilyichev (U. S. S. R.) S. Prakash (India) F. E. Richart, Jr. (U. S. A.)
Members of the Panel/Membres du Groupe de Discussion: S. Hansbo (Sweden) M. Novak (Canada)
T. Shibata (Japan) P. W. Taylor (New Zealand)
Session Secretary/Secrétaire de Session: Y. Sugimura (Japan)

Chairman: H.B. Seed

On behalf of the Organizing Committee for this 9th International Conference on S.M. and F.E. I would like to welcome you to Session 4 on the subject of Soil Dynamics and its Application to Foundation Engineering. I should note that we are making history at this session since it is the first time that the subject of Soil Dynamics has been accorded feature status as a topic for one of the Main Sessions.

This branch of Geotechnical Engineering has undergone a rapid development in recent years, as evidenced by the fact that approximately 20% of the papers contributed to this Conference fall in this subject area. Only eight years ago the number was just a fraction of this, and it was in a Specialty Conference on Soil Dynamics at Mexico City in 1969 that many members of the Society were first made aware of the increasing interest and activity in this important field.

Prior to the mid-sixties, studies of soil dynamics usually dealt with problems of blast loading or foundation vibrations. In the period 1959 to 1971, however, a series of dramatic failures in earth structures during earthquakes made it increasingly apparent that attention had to be given to the soil mechanics aspects of this environmental hazard. It was not easy to ignore the problems posed by, for example:

1. The dramatic subsidence of an island near Valdivia in the Chilean earthquake of 1959.

2. Settlements of backfills adjacent to bridge abutments in the 1964 Alaska earthquake, the 1964 Niigata earthquake and the 1971 San Fernando earthquake.

3. The dramatic effects of soil liquefaction, starting with sand boils and ultimately leading to overturned structures, the floating of buried structures to the ground surface and enormous damage to buildings in the 1964 Niigata earthquake in Japan.

4. The enormously damaging landslides in the 1964 Alaska earthquake, which carried away strips of coastline at Seward, Valdez, Anchorage and other areas through flow slides clearly reminiscent of those which had occurred in Kansu Province, China in 1920 and in the Chait earthquake in Russia in 1944.

5. The devastating debris slide in the 1969 Peruvian earthquake where over 50 million cubic yards of soil and ice rushed down a mountainside at over 200 miles per hour, jumped over a 500 ft. high ridge of cliffs and virtually buried the town of Yungay, and most of its 22,000 inhabitants.

6. The major slide in the upstream slope of the Lower San Fernando Dam in an earthquake about 30 miles north of Los Angeles in 1971. The slide removed the upper 30 ft. of the embankment, leaving only about 5 ft. of soil separating the water in the reservoir from thousands of people living in lowlying areas immediately downstream. The extent of the slide, which became increasingly apparent as the reservoir was emptied, and the near brush with what might easily have been the greatest natural disaster in the history of the United States (if the earthquake had been only a little stronger, if there had been a fairly strong aftershock, or even if the earthquake had occurred on some other day when the reservoir level was somewhat higher) made it imperative to find some means of anticipating in advance of their occurrence, potentially disastrous effects of this type.

7. The subtle relationships, often called soil-structure interaction, which can lead to enormous differences in building performance during earthquakes depending on the nature of the structure and the characteristics of the soils underlying its foundations; nowhere was the potential for building damage more dramatically apparent than in the Managua earthquake of 1973 and nowhere have the effects of soil structure interaction been more dramatically demonstrated than by the damage statistics in the Caracas earthquake of 1967.

These events and the need to understand them, coupled with increasing national needs for

construction of critical structures such as nuclear power plants, large oil and gas pipelines, and off-shore structures for which dynamic effects are introduced by wave action, have led to progressively increasing activity in areas of soil dynamics involving studies of soil behavior under cyclic stress applications, dynamic stabilization techniques to prevent detrimental performance, ground response to earthquake excitation, soil-structure interaction effects and pile-structure interaction effects.

Fortunately the Organizing Committee appointed a highly qualified group of general reporters to review the accomplishments to date in these various areas, a leading figure in the field to present the general report this morning and a distinguished panel to supplement the general report and respond to any questions you may wish to raise.

The State-of-the-Art report was prepared by Professor Yoshiaki Yoshimi of the Tokyo Institute of Technology, Professors F.E. Richart and S. Prakash, and Drs. D.D. Barkan and V.A. Ilyichev. It is with the greatest of pleasure that I now introduce Professor Yoshimi, who has contributed enormously to current knowledge of soil dynamics, to present the State-of-the-Art report and provide you with information on the progress made to date in dealing with some of the problems I have just described and others falling within the general area of Soil Dynamics. Professor Yoshimi.

General Reporter: Y. Yoshimi

(The General Reporter's presentation is omitted here because it is essentially the same as the contents of the State-of-the-Art Report in Proceedings Volume II and of the General Report in Proceedings Volume III.)

Chairman Seed

I am now going to ask one of professor Yoshimi's Co-Reporters, Professor Richart, to add any supplementary observations he wishes to make to the State-of-the-Art Report as it has been presented.

Co-Reporter: F.E. Richart, Jr.

My comments relate to laboratory evaluations of dynamic soil properties, particularly to the shear modulus, G, and the extrapolation of laboratory data for analysis of field problems.

A convenient method for determining the dynamic shear modulus in the laboratory is the resonant column method. This method was based on early research by Iida (1938) in Japan, and it has been developed rapidly during the past two decades. At the present time I estimate that there are 75 to 80 resonant column devices throughout the world, - 8 are in Japan.

Laboratory studies permit convenient studies of the various parameters which affect the value of the shear modulus, G (see Richart, Hall, and Woods, 1970, Chap. 6, for example). My comments here are limited to the effects of shearing strain amplitude and time, and their interaction, on G.

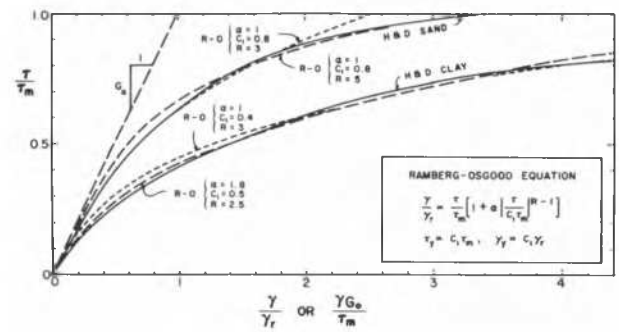

Fig. 1 Hardin-Drnevich dimensionless curves for sands and clays, and Ramberg-Osgood fitted curves

Figure 1 shows two curves developed from test data by Hardin and Drnevich (1972), one for tests on sands and one for tests on clays. The test data for each material collapses onto one curve when plotted on dimensionless diagrams having the ratio τ (shearing stress) divided by τ_{max} (ultimate shearing stress) as ordinate, and γ (shearing strain) divided by γ_r (the reference shearing strain) as abscissa. The reference shearing strain, γ_r, is obtained by dividing τ_{max} by the low-amplitude shear modulus, G_o. The reference strain is an important factor in determining dynamic stress wave transmissions through soils.

Table 1. Reduction of Shear Modulus at 5 and 25 Meters Depth in Sand Caused by Shearing Strain Amplitude of 0.001

Depth (m)	τ_{max} (kg/cm^2)	G_o (kg/cm^2)	γ_r	γ/γ_r	G/G_o
5	0.28	750	3.7×10^{-4}	2.70	0.37
25	1.40	1690	8.2×10^{-4}	1.22	0.61

Table 1 illustrates the importance of evaluating the ratio of the actual shearing strain in the soil with respect to the reference strain. For a given shearing strain of 0.001 at depths of 5 and 25 meters in a deposit of sand, the ratio of γ/γ_r is 2.7 at 5 meters, and 1.22 at 25 meters. The corresponding ratios of G/G_o are 0.37 at 5 meters and 0.61

at 25 meters, as obtained from Fig. 2. Therefore the same actual value of shearing strain represents a greater decrease in stiffness at shallower depths in sands.

The test data plotted on the dimensionless diagram with G/G_o as ordinate and γ/γ_r as abscissa as shown on Fig. 2 are usually obtained at the end of one day's testing time for cohesive soils, and at a shorter time for sands. It has been recognized for many years that there are definite time effects associated with laboratory tests for dynamic shear modulus. Even for the best "undisturbed" field samples, stress changes occur during unloading, trimming, and reloading, as well as by handling. Upon reloading in the test apparatus the field stress conditions are not reproduced exactly, therefore

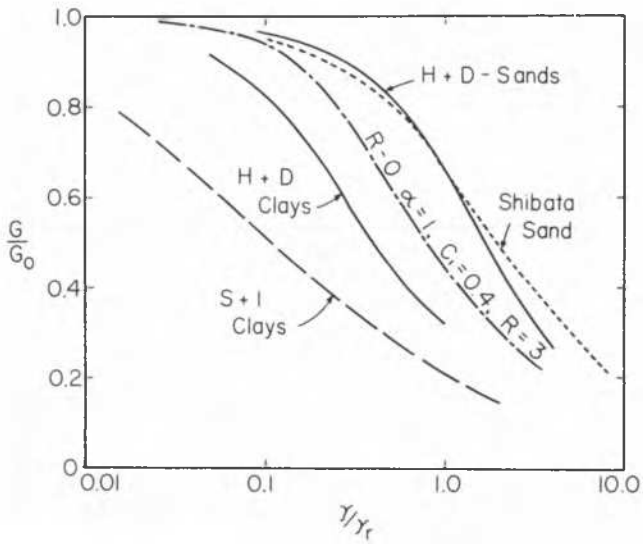

Fig. 2 Dimensionless curves for shear modulus reduction with increasing shear strain

readjustments occur during the reloading process. These effects may be evaluated by intermittent vibration tests throughout the testing period. Most tests on cohesive soils show a rapid increase in shear wave velocity during primary reconsolidation, followed by a linear increase in shear wave velocity with logarithm of time during a secondary behavior. Figure 3 shows typical test curves for sands, overconsolidated clays, and for normally consolidated clays. Note that the secondary time effect is insignificant for sands, but that it can be important for clays.

Figure 4 illustrates the use of the secondary time effect to extrapolate laboratory test data to field conditions. Comparisons of the low strain amplitude shear modulus from field tests with laboratory data including time effects have shown good agreement (see Anderson and Woods, 1975, for example). For higher shearing strain amplitudes, laboratory

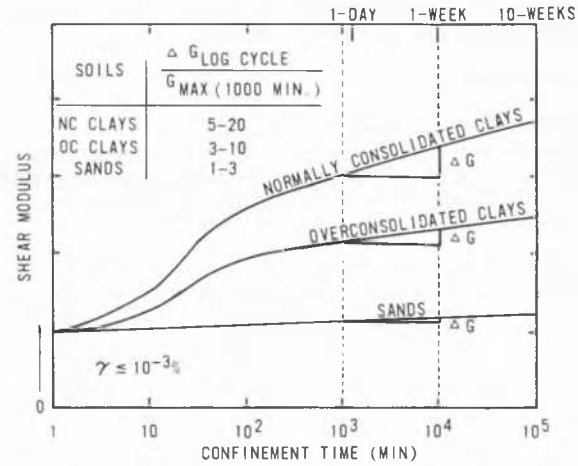

Fig. 3 Effect of confinment time on shear modulus

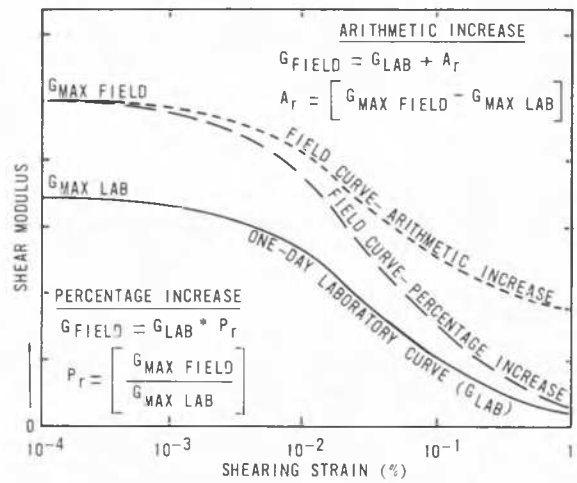

Fig. 4 Field curve predicted by arithmetic and percentage increase in modulus

tests have shown essentially the same secondary time effects as those found at low shearing strain amplitudes. Therefore our recommendation is to use an arithmetic (constant interval) adjustment of laboratory data to account for the secondary time effects, rather than a constant percentage increase. A more complete discussion of this topic was given by Richart, Anderson, and Stokoe (1977).

In conclusion, we believe that the secondary time effects are important and can be evaluated by laboratory tests. These effects most likely occur in the field also because of stress changes during excavation and con-

struction. I recommend that field measurements of shear wave velocity changes with time be evaluated beneath newly constructed foundations on cohesive soils.

REFERENCES

Anderson, D.G. and Woods, R.D. (1975), "Comparison of Field and Laboratory Shear Moduli," Proc. Conf. on In Situ Measurements of Soil Properties, N. Carolina State Univ., Raleigh, N.C., Vol. 1, pp. 69-92.

Hardin, B.O. and Drnevich, V.P. (1972), "Shear Modulus and Damping in Soils: Design Equations and Curves," J. SMFD, Proc. ASCE, Vol. 98, No. SM7, pp. 667-692.

Iida, K. (1938), "The Velocity of Elastic Waves in Sand," Bull. ERI, Vol. 16, pp. 131-144.

Richart, F.E., Jr., Anderson, D.G., and Stokoe, K.H., II, (1977), "Predicting In Situ Strain-Dependent Shear Moduli of Soil," Proc. VI WCEE (New Delhi).

Richart, F.E., Jr., Hall, J.R., Jr., and Woods, R.D. (1970), Vibrations of Soils and Foundations," Prentice-Hall, Inc., Englewood Cliffs, N.J. (Japanese translation by T. Iwasaki and A. Shimazu, 1975, Kajima Inst. Publ. Co., Ltd., Tokyo).

Chairman Seed

I would now like to invite our panelists to comment on the remarks made by the state-of-the-art reporters to date. Professor Taylor.

Panelist: P.W. Taylor

Non-Linear Dynamic Stress-Strain Relationships and Their Application

It is now fully accepted that the dynamic stress-strain relationships, for soils, are almost independent of frequency over a wide range (0.1 to 10 Hz) but are strongly amplitude dependent. Load deformation graphs from a dynamic triaxial test are shown in Fig. 1. The hysteresis loops for cycles of reducing strain amplitude clearly show the non-linear behaviour. The results of a similar test but with asymmetrical strain cycles are shown in Fig. 2.

At the University of Auckland (New Zealand) we use a free vibration torsion test to determine the relationship, for saturated clays between the hysteresis shear modulus, G, and the shear strain amplitude, γ. The apparatus is shown diagrammatically in Fig. 3.

The sample acts as a torsion spring whose stiffness, related to the moment of inertia of the system, determines the frequency of oscillation. (Ref. Taylor and Parton, 1973.) From the record of oscillation, such as that

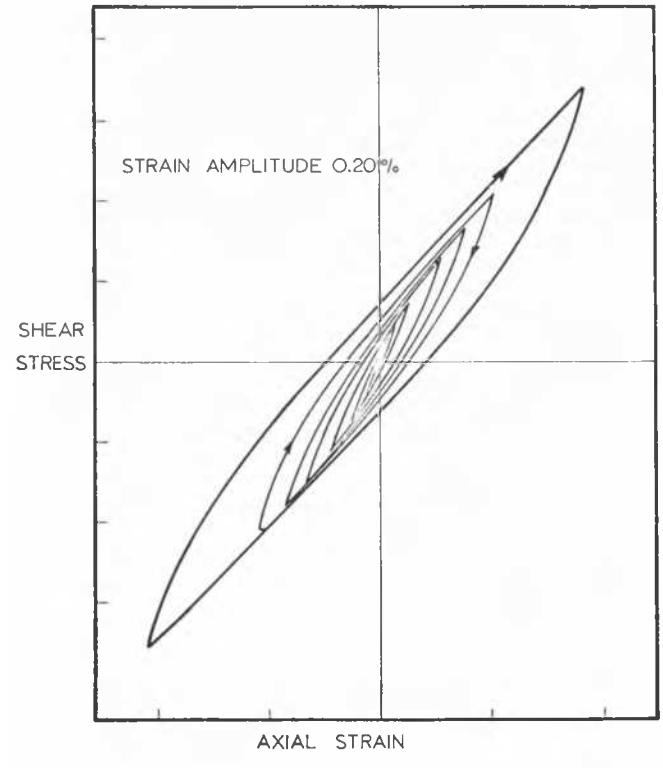

Fig. 1 Hysteresis loops—reducing strain amplitudes

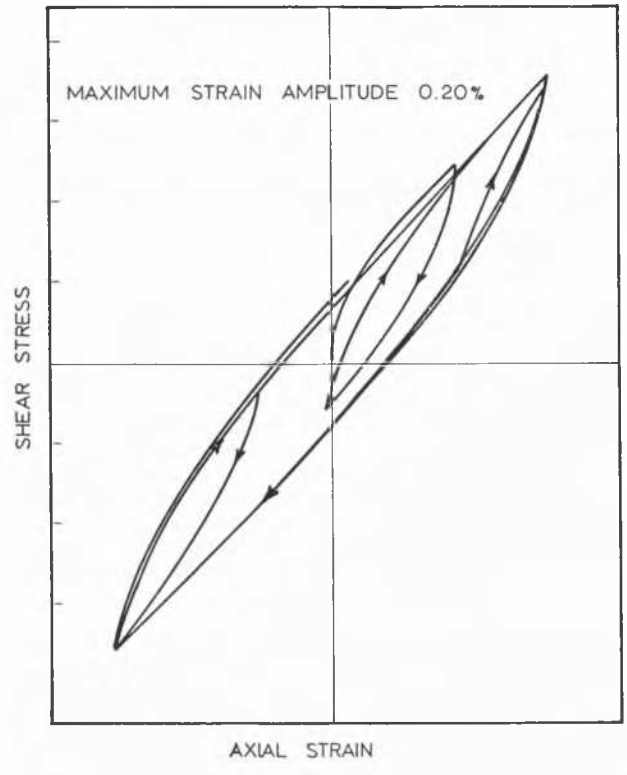

Fig. 2 Hysteresis loops—asymmetrical strain cycles

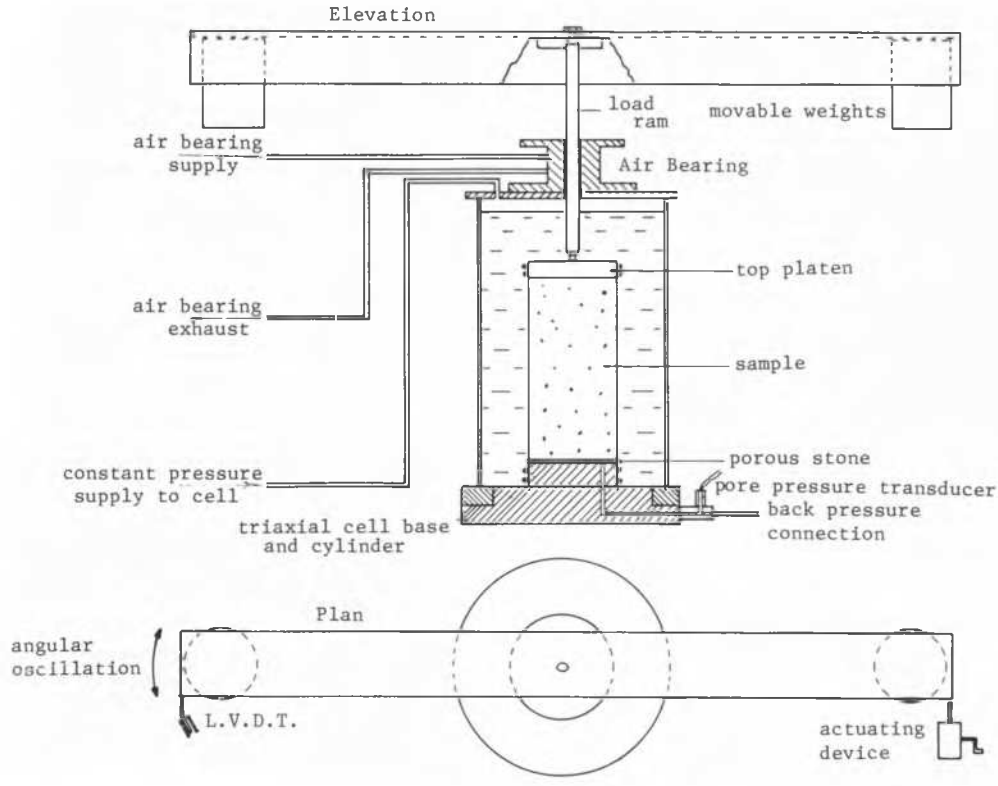

Fig. 3 Free vibration torsion apparatus

shown in Fig. 4, the frequency and amplitude of each cycle may be found and relationship between shear modulus and strain amplitude determined.

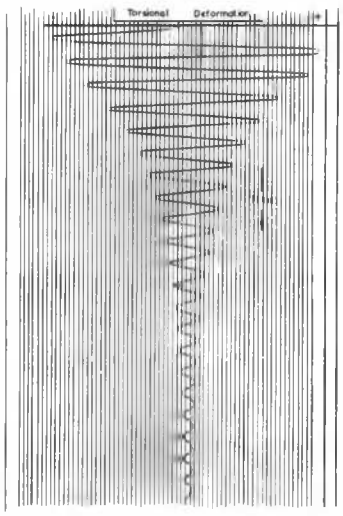

Fig. 4 Oscillation record

The fact that dynamic soil properties are amplitude-dependent rather than frequency-dependent suggests that the energy loss mechanism is not viscous. The model we have developed comprises a number of elastoplastic elements each with a spring (stiffness k) and a Coulomb resistant (R) in series. The basic characteristics of such an "elasto-plastic element" are illustrated in Fig. 5.

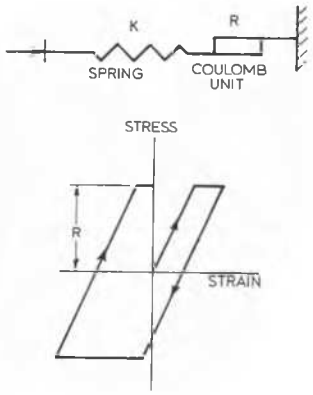

Fig. 5 The elastoplastic element

A number of these elastoplastic elements in parallel, with different k and R values form a Masing system which reproduces the hysteresis loops of clays as closely as may be desired. It appears to correspond with the micro-mechanisms operating within the clay. It can be seen from Fig. 6 that, even with only three elements, the modulus decreases and the energy loss increases with increase in strain amplitude. In this way, the stress-strain relationships for a soil can be closely reproduced. The result is summarised in Fig. 7. This is similar to that postulated by Hardin and Drnevich, 1972. In practice, for site response analysis, we use about 10 such elements for each significantly different soil layer. The shear modulus/strain amplitude relationship found in the laboratory must first be corrected for sample disturbance effects. This is done by reference to down-hole shear-wave velocity measurements. In my opinion this method should be used in preference to making a "secondary time correction."

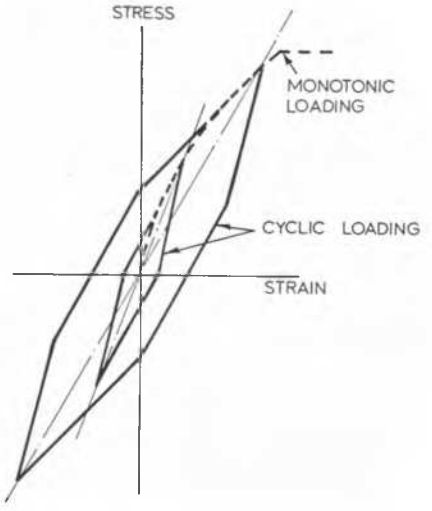

Fig. 6 Hysteresis loops for three elastoplastic elements in parallel

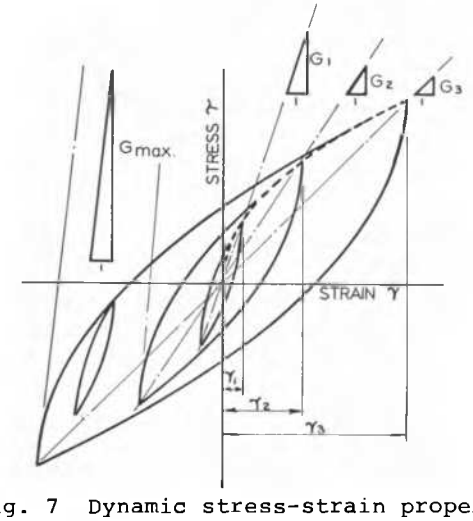

Fig. 7 Dynamic stress-strain properties of soils

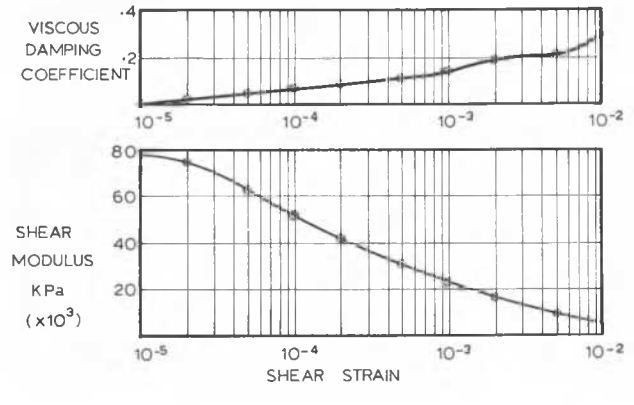

Fig. 8 Typical modulus amplitude relationship

Fig. 8 shows a typical relationship between shear modulus, G, and shear strain amplitude, γ. The model parameters (k and R values) are then determined.

At each of the 10 points shown the model will reproduce exactly the modulus appropriate to that amplitude. (The range covered is 10^{-5} to 10^{-2}.) Hysteretic damping is inherent in the model and is shown (as an equivalent viscous damping factor) in the upper part of the diagram. Using a lumped-mass, numerical method developed by Larkin (1977) we are now carrying out site response analyses and the results are significantly different from those using a linear visco-elastic approach, as shown in Fig. 9.

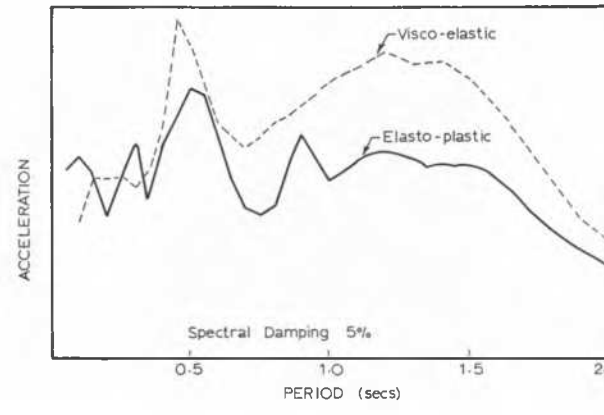

Fig. 9 Surface response spectra

While, in the linear visco-elastic method, some attempt is made to allow for non-linear effects by applying iteration until the soil modulus is appropriate for the "average" strain in the soil, the final analysis is made using a linear viscously-damped system.

There are, currently, a number of investigators using non-linear methods. Significant work has been done at the University of California, Berkeley, and in the use of the Ramberg-Osgood model for the "characteristics" method at the University of Michigan.

In my opinion, the most promising current developments are those where non-linear relationships are derived from fundamental soil properties. In the paper by M.J. Pender to this Conference, the Cambridge model for clay (Cam-clay) is extended to cyclic loading. For sands, the work described by Finn, Lee and Martin at this Conference, wherein build-up and dissipation of pore pressure can be described, shows great promise.

REFERENCES

Taylor, P.W. and Parton, I.M., "Dynamic Torsion Testing of Soils", Proc. 8th International Conf. on Soil Mechs. and Found. Eng. v.1, p. 425 (Moscow, 1973).

Hardin, B.O., and Drnevich, V.P., "Stress Modulus and Damping in Soils: Measurement and Parameter Effects", Jour. Soil Mechs. and Founds. Div., ASCE, v.98, No. SM6 pp. 603-624 (1972).

Larkin, T.J., "Propagation of Seismic Waves through Non-Linear Soil Media", University of Auckland, School of Engineering Report No. 144 (1976).

Pender, M.J., "Modelling Soil Behaviour under Cyclic Loading", Proc. 9th International Conf. on Soil Mechs. and Found. Eng., v.2, p. 325 (Tokyo 1977).

Finn, W.D.L., Lee, K.W., and Martin, G.R., "Dynamic Effective Stress Analysis of Sands", Proc. 9th International Conf. on Soil Mechs. and Found. Eng., v.2, p. 231 (Tokyo 1977).

Chairman Seed

Are there any other panelists who would like to comment on this subject? Professor Shibata.

Panelist: T. Shibata

The following comments are concerned with the dynamic stress-strain relations of clays: in particular, the simple and practical expressions for dynamic behavior of clays which are obtained on the basis of our recent study.

Many attempts have been made to obtain the analytical expressions for nonlinear stress-strain relations of soils under cyclic loading conditions. Typical expressions among them are known by the name of bi-linear, Ramberg-Osgood and Hardin-Drnevich models. The equations proposed by Ramberg and Osgood (1943) have been applied to the structural problems in 1960's, and to soils in the 1970's. On the other hand, Hardin-Drnevich (1970) developed the basic relationships for the variations of shear modulus and damping with strain amplitude, on the basis of hyperbolic stress-strain relation. Our time is limited, so I will proceed directly to the new stress-strain model based on the effective stress.

The results of cyclic loading tests on soft clays indicate a degradation in the soil stiffness due to cyclic loading. This effect is associated with an increase in pore pressure, i.e., a decrease in effective confining pressure. Fig. 1(a) shows the cyclic loading test with constant-strain-amplitude. Under this cyclic loading test, the effective confining pressure, σ_o, gradually decreases with the number of cycles as shown in Fig. 1(b). Due to the decreasing of σ_o', the backbone curve degrades and adopts a position lower than the initial curve as shown in Fig. 1(c). In Fig. 1(c) are also shown the stress changes during a constant-strain-amplitude test; the shear stress will decrease with cyclic number as noted by the arrow marks.

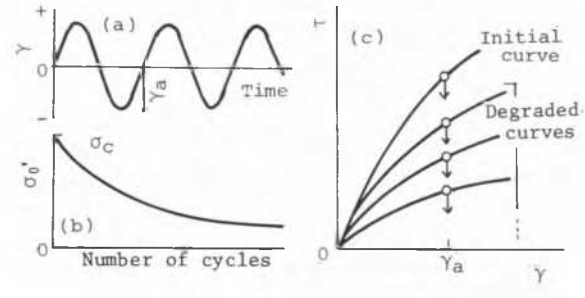

Fig. 1 (a) Cyclic loading test with constant strain amplitude, (b) decreasing of effective confining pressure, (c) Degradation of backbone curve

The initial backbone curve is assumed to be expressed by Eq. (1), which is the same expression of Hardin-Drnevich model,

$$\frac{\tau}{\gamma} = \frac{G_o \cdot \tau_f}{\tau_f + G_o \cdot \gamma} \qquad (1)$$

where G_o is the initial or maximum shear modulus; and τ_f is the shear strength. And the degraded curves are supposed to be given by Eq. (2).

$$\frac{\tau}{\gamma} = \frac{G_o' \cdot \tau_f'}{\tau_f' + G_o' \cdot \gamma} \qquad (2)$$

where G_o' and τ_f' are the initial shear modulus and shear strength of degraded curves, respectively: they are assumed to be decreased with the decreasing of effective confining pressure. Taking the inverse of both sides in Eq. (2),

$$\frac{\gamma}{\tau} = \frac{1}{G_o'} + \frac{\gamma}{\tau_f'} \qquad (3)$$

Multiplying both sides of Eq. (3) by the effective confining pressure σ_o', and with some rearrangement, Eq. (4) may be obtained.

$$\frac{\sigma_o'}{\tau} = \left(\frac{\sqrt{\sigma_o'}}{G_o'}\right)\left(\frac{\sqrt{\sigma_o'}}{\gamma}\right) + \frac{\sigma_o'}{\tau_f'}$$

$$= \frac{1}{\alpha}\left(\frac{\sqrt{\sigma_o'}}{\gamma}\right) + \frac{1}{\beta} \qquad (4)$$

where $\alpha = G_o'/\sqrt{\sigma_o'}$, $\beta = \tau_f'/\sigma_o'$

Eq. (4) indicates the relationship between shear stress τ, strain γ and effective confining pressure σ_o'. Therefore, if the degraded backbone curve is shown in the form of τ/σ_o' vs $\gamma/\sqrt{\sigma_o'}$ plot, these degraded backbone curves are shown to become uniquely determined as in Fig. 2. The initial tangent of the curve is defined as α and the asymptote is β.

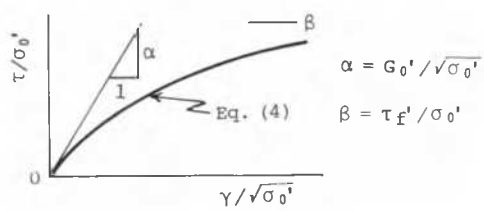

Fig. 2 Representation of degraded backbone curve

Now the following discusses the validity of a rather simple expression of Eq. (4) by experimental results. Taylor and Bacchus (1969) reported the results of strain-controlled cyclic triaxial tests on cohesive soil with pore water pressure measurement. Fig. 3(a) is reproduced from the results of one of these tests: the shear stress changes during 30 cycles for normally-consolidated samples are plotted against the cyclic shear strain γ. From this figure it will be seen that the stress-strain relation is not uniquely determined but that the stress decreases with an increase of the number of cycles. The shear stresses corresponding to 30 cycles are smaller than that of one cycle. Next, the above results are replotted in Fig. 3(b) in order to verify the proposed Eq. (4). Fig. 3(b) shows the relationship between σ_o'/τ on the left side in Eq. (4) and $\sqrt{\sigma_o'}/\gamma$ of the first term on the right side. The results shown in this figure are scattered, but they appear to indicate that a linear relationship exists.

Next, a series of cyclic tests on remolded and reconsolidated clays were made by using varying values of cyclic strain. Fig. 4(a) shows the time history of strain amplitude used in this test. This time history was

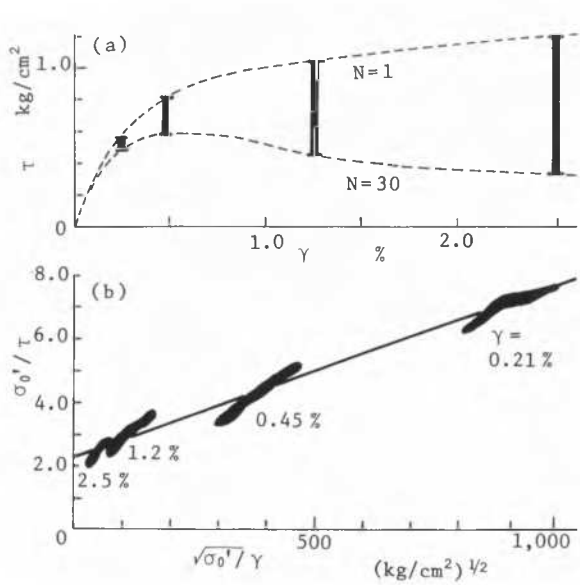

Fig. 3 (a) Shear stress vs. cyclic strain (Taylor and Bacchus, 1969), (b) Comparison of Eq. (4) with experiments

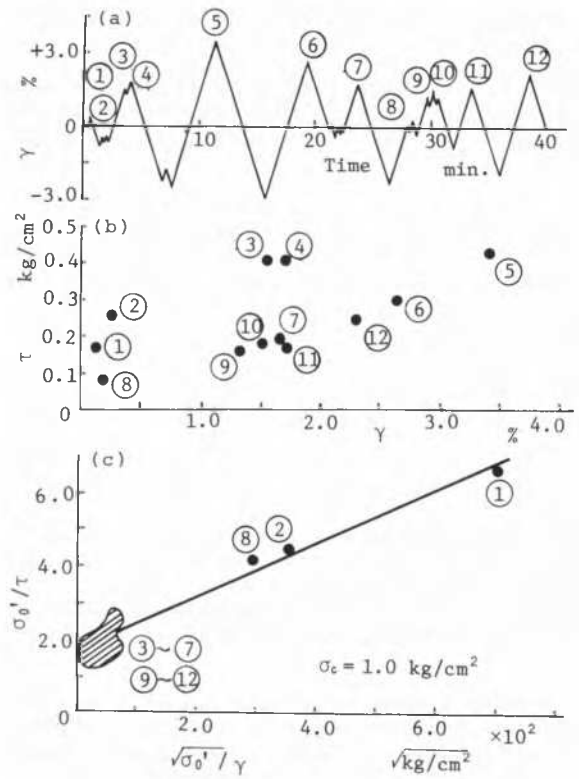

Fig. 4 (a) Time history of strain amplitude, (b) shear stress vs. cyclic strain, (c) comparison of Eq. (4) with experiments

obtained on the basis of the acceleration record during the Tokachioki earthquake in 1968. The cyclic shear stress τ was measured at different cycles and the results are plotted in Fig. 4(b). The numbers enclosed by circles correspond to the peak points of strain amplitude in Fig. 4(a). From this figure, it is seen that the stress-strain relation is not uniquely determined, and that the effect of degradation is very pronounced in this test.

The above results are replotted in Fig. 4(c) to verify the proposed effective stress model in the form of σ_o'/τ and $\sqrt{\sigma_o'}/\gamma$ plot. The numbers enclosed by circles are also corresponding to the peak points of the strain amplitude as shown in Fig. 4(a). The results are scattered, especially for the ranges of higher strain amplitudes (the cross-hatched part), but they appear to indicate that a linear relation exists. Thus the validity of the new soil model is confirmed for transient cyclic loading.

REFERENCES

Ramberg, W. and Osgood, W.T. (1943), Description of Stress-Strain Curves by Three Parameters, Tech. Note 902, National Advisory Committee for Aeronautics.

Hardin, B.O. and Drnevich, V.P. (1970), Shear Modulus and Damping in Soils: Measurement and Parameter Effects, Tech. Report UKY 26-70-CE2, Univ. of Kentucky.

Taylor, P.W. and Bacchus, D.R. (1969), Dynamic Cyclic Stress Tests on Clay, Proc. 7th I.C.S.M.F.E., Vol. 1, Mexico, pp. 401-409.

Chairman Seed

I think we should terminate this discussion now of stress-strain properties which has occupied much of our discussion this morning, and turn to a new topic. Therefore, I am going to ask Dr. Ilyichev if he has any remarks to add to the state-of-the-art presentation as it was made earlier.

Co-Reporter: V.A. Ilyichev

I would like to draw your attention to one of the relatively new branches in soil and foundation dynamics which permits to predict vibrations of foundations and surrounding structures and ground.

It is well known that the behavior of the ground is nonlinear. But in very many cases the dynamic system consisting of foundation and ground is almost linear under the moderate industrial dynamic loads and can be considered as linear even when we observe a long-term settlement due to vibrations. Most practical design methods are also linear. Restricting by that linear condition it is possible to improve the existing methods for prediction of vibration level of foundations and structures.

This improvement may be based on the powerful and deep studied theory of linear differential equations and the main idea coincides with the assumption of so-called "black box" in the cibernetics. We don't know the inner structure of such a complicated system as ground. But we can calculate the behaviour of this unknown system if we know the response of it on a special standard unit load, instantaneous impulse, or harmonic force.

I will illustrate that approach with the simplest examples. Let us consider vertical vibration of foundations. For many well-known mathematical models of the ground we can calculate these transient and harmonic responses and then make a prediction. There are many papers realizing this way. But there is no model which describes the real ground condition.

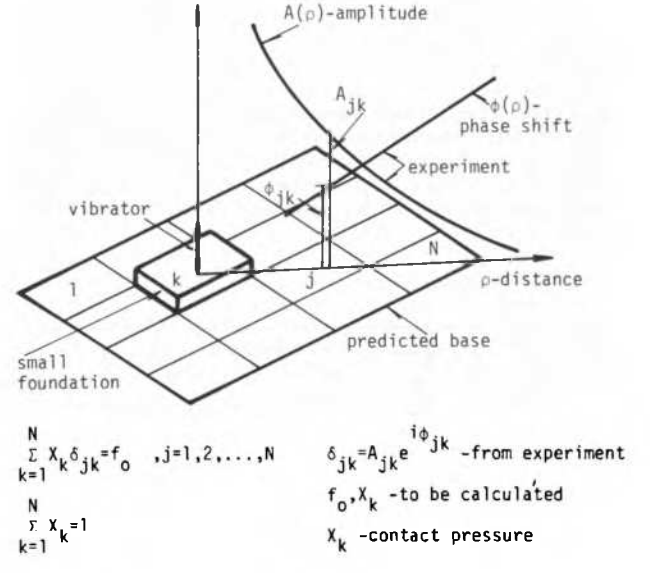

$$\sum_{k=1}^{N} X_k \delta_{jk} = f_o \quad ,j=1,2,\ldots,N \qquad \delta_{jk}=A_{jk}e^{i\phi_{jk}} \text{ -from experiment}$$

$$\sum_{k=1}^{N} X_k = 1 \qquad f_o, X_k \text{ -to be calculated}$$

X_k -contact pressure

The proposed idea is that the unit response of the system is not calculated theoretically but measured in situ, and then we operate with the unit response functions in usual manner. The experimental procedure has its own specifics and difficulties, but its results may be very useful. For example, we can calculate the contact stresses, foundation amplitude and then in similar way also a vibration level of any other objects.

So there is a possibility to provide a very cheap experiment with the small foundation and then to predict by calculation the behavior of the real foundation. The examples of the prediction are in the State-of-the-Art Report. The footing area of small foundations may be in 10 to 50 times less than the footing area of the real foundation.

The proposed method can catch unexpected detail of foundation behavior which cannot be explained by the theory of elastic homogeneous

half-space. Also, this method can precalculate experimentally observed reduction of the rigidity coefficient while the footing area increases.

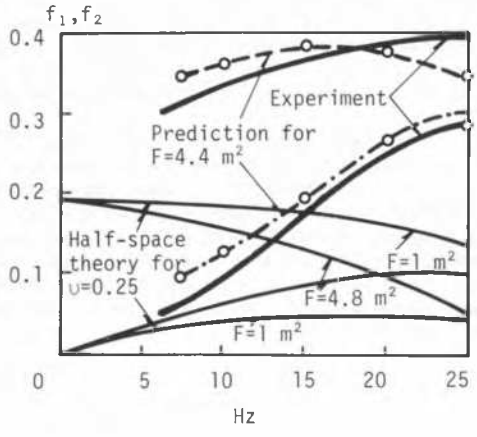

Using the mentioned approach it is not necessary to introduce such terms as ground model, rigidity coefficient, damping coefficient, added soil mass, and so on. But we can certainly use them if we want. That approach

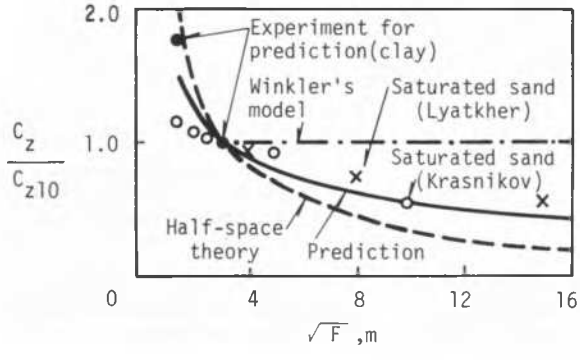

was also experimentally proved by Svinkin for prediction of ground vibration around hammers and other machines. I hope that this method under consideration may be useful during design of large foundations and construction sites with heavy dynamic equipment.

Chairman Seed

Would any of the panelists like to discuss this subject? Professor Novak.

Panelist: M. Novak

I would like to discuss a few points raised in part 4 of the State-of-the-Art Report dealing with dynamics of bases and foundations.

The first point concerns the ability of theoretical models to predict dynamic response of footings. The authors state that large differences are often observed between the theoretically predicted resonant frequencies and amplitudes and corresponding experimental values. As an example, they mention the underestimation of vertical resonant amplitudes by a factor of 2 to 5.

Such differences indeed exist and were observed by a few others including the writer. In the first evaluation of the experiments conducted with surface and embedded footings at The University of Western Ontario, the vertical response was underestimated typically by a factor of two while coupled horizontal response and torsional response were overestimated by several hundred percent. However, later evaluation based on improved theories revealed that the discrepancy could be considerably reduced if soil layering and material damping are included. An example of this is shown in Fig. 1 in which the experimental resonant amplitudes of coupled response to horizontal excitation are compared with theoretical values calculated with and without soil material damping. This damping is

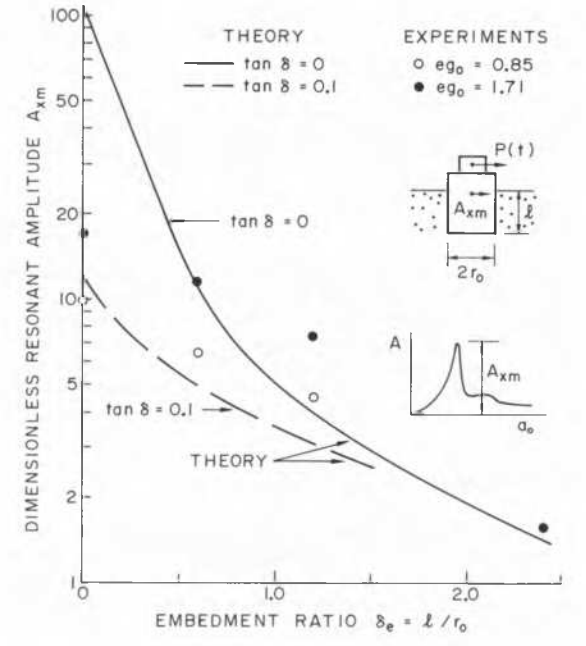

Fig. 1 Comparison of theoretical and experimental resonant amplitudes of coupled response to horizontal excitation

characterized by tanδ where δ = loss angle. The experiments are described in Novak and Beredugo (1971). The resonant amplitudes were measured at the first resonance and the test bodies were embedded to different depths, ℓ. (The difference between the full and void

circles is due to nonlinearity.) For surface footings ($\ell/r_o = 0$) the theory overestimates the experimental values quite dramatically if soil material damping is ignored. This is a result of the very low geometric damping associated with this vibration mode.

Good agreement between experiments and theory was also reported recently by a few other authors. Excellent agreement was found by Tajimi et al. (1977), fair agreement was achieved by Kobori et al. (1972) and a very good prediction of resonant frequencies was obtained by Petrovski (1977). All of this indicates that, despite many defficiencies of the theories, significant progress can be made by improving the capability of the theoretical models.

The second point concerns the procedure suggested for the determination of the compliance functions f_1 and f_2 by means of in situ experiments conducted with test bodies much smaller than the prototype.

It may be that such a procedure gives satisfactory results under certain conditions. However, the field experiments with small test bodies cannot be considered a panacea for the inadequacy of the theory because the conditions of physical and even geometrical similarity between the model and the prototype are not in general satisfied. As an example, consider a deposit of sand overlying bedrock (Fig. 2). For the test body, the ratio h/d_1 is large, say ten and the soil deposit behaves like a half-space at small $a_o = r_o\omega/V_s$. The prototype has $h/d_2 = 1$ and the soil deposit behaves like a layer at large a_o featuring layer resonances, much

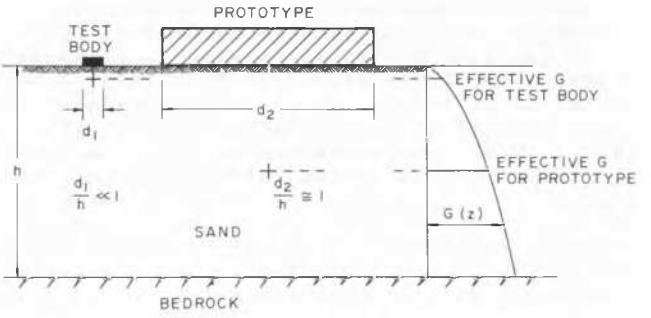

Fig. 2 Differences between test body and prototype

smaller geometric damping etc. Obviously, the condition of geometric similarity requires $d_1/h = d_2/h$. In addition, the shear modulus of sand increases with confining pressure (depth) and therefore, the effective shear modulus is much smaller for the test body than it is for the prototype. The similarity is further aggravated by the effect of embedment (also depending on confining pressure) and differences in strain levels. These factors are well recognized by many researchers and lead to the development of some sophisticated experimental techniques such as model investigations in large centrifuges.

Finally, it may be noted that progress has been made in understanding the dynamic behavior of piles and predicting their dynamic stiffness and damping. This is evident from some contributions to the Main Session No. 4

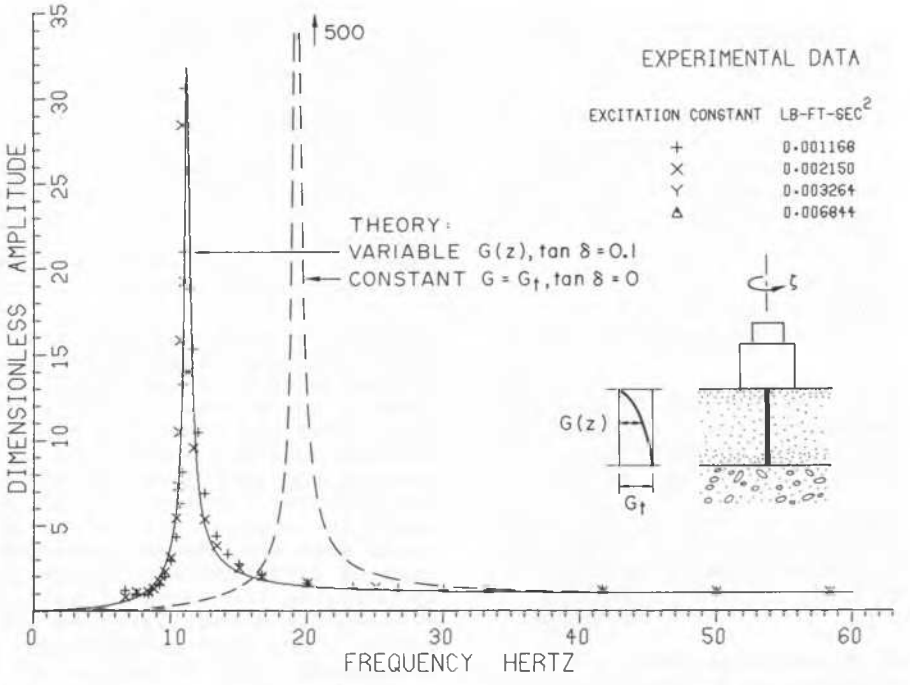

Fig. 3 Comparison of theoretical and experimental responses of pile foundation in torsion ($A = mgu_o / eg_o$)

and the Specialty Session No. 10. The variation of soil properties with depth is very important for piles also. This factor can be included in the finite element approaches (Kuhlemeyer, 1976; Blaney et al., 1976; Tajimi et al., 1976, 1977) or approximate analytical solutions (Novak and Aboul-Ella, 1978). This is exemplified by Fig. 3 which shows the improvement in the theoretical prediction of the response of a pile foundation that can be achieved if the variation of soil properties with depth is accounted for. With torsion, the inclusion of material damping of soil is also essential.

It can be expected that further progress will result from making the theories better able to accommodate realistic soil properties and their variation with depth and strain and from learning more about dynamic properties of soil.

REFERENCES

Blaney, G.W., Kausel, E. and Roesset, J.M. (1976). "Dynamic Stiffness of Piles", Proceedings of the Second International Conference on Numerical Methods in Geomechanics, held at Virginia Polytechnic Institute and State University, Blacksburg, Virginia, U.S.A., June, 1976, published by ASCE, New York, pp. 1001-1012.

Kobori, T., Minai, R., Suzuki, T. and Kusakabe, K. (1974). "Dynamic Characteristics of Soil-Foundation Systems Detected From Oscillator Tests - Part 1 Nonelastic Dynamic Characteristics", Annual Bull. of the Dis. Prev. Res. Institute, Kyoto University, pp. 1-24.

Kuhlemeyer, R.L. (1976). "Static and Dynamic Laterally Loaded Piles", Res. Report No. CE 76-9. Dept. Civ. Engrg., Univ. Calgary, Calgary, Alta., Canada, p. 48.

Novak, M. and Beredugo, Y. (1971). "The Effect of Embedment on Footing Vibrations", Proceedings of the First Canadian Conference on Earthquake Engineering, May 1971, University of British Columbia, Vancouver, Canada, pp. 111-127.

Novak, M. and Aboul-Ella, F. (1978). "Vibration of Piles Embedded in Layered Media", Journal of the Engineering Mechanics Division, ASCE, (to appear).

Petrovski, J. (1977). "Prediction of Dynamic Response of Embedded Foundation", Proceedings of the 6th World Conference on Earthquake Engineering, New Delhi, Vol. 4, pp. 169-174.

Tajimi, H. and Shimomura, Y. (May 1976). "Dynamic Analysis of Soil-Structure Interaction by the Thin Layered Element Method", Transactions of the Architectural Institute of Japan, No. 243, pp. 41-51. (In Japanese.)

Tajimi, H., Minova, C. and Shimomura, Y. (1977), "Dynamic Response of a Large-Scale Shaking Table Foundation and Its Surrounding Ground", Proceedings of the 6th World Conference on Earthquake Engineering, New Delhi, Vol. 4, pp. 61-66.

Chairman Seed

Thank you Professor Novak. I am now going to ask Professor Prakash to make whatever statements he wishes to add to the State-of-the-Art Report, and then Professor Hansbo to discuss whatever discussion he wishes to make. And then we declare a short recess for whatever time we need to reevaluate how much time we should have for discussions from the floor. Professor Prakash.

Co-Reporter: S. Prakash

Some Unusual Aspects of In Situ Testing of Soils

In situ testing forms are essential feature of any important geotechnical exploration programme aimed at evaluating design parameters for analysis of a soil-structure-interaction problem. Most of the field tests and testing techniques are well established. However typical soil conditions and site locations may necessitate special in situ tests which have to be suitably planned and carefully interpreted. The author has been associated with a large number of important geotechnical investigations in India. At one of the sites for a proposed cement factory where the soil consisted of gravels and boulders with fine matrix and the area was seismically active, it became essential to ascertain the qualitative and quantitative aspects about the behaviour and strength of boulder deposits under dynamic loads. In addition to the tests such as vertical and horizontal plate load tests, block vibration tests and wave propagation tests, dynamic passive pressure tests on vertical reinforced concrete walls 1.5m high, 1.0m wide and 0.3m thick cast in pits 1.5m deep were therefore conducted. In order to isolate the test wall from possible side effects from the pit, side walls, 0.5m long were constructed in brick masonry.
Reaction walls of the same size as the test walls were made opposite to them.

The static loads were applied to the test walls through a loading frame and a calibrated hydraulic jack at 1/3 height above base. The dynamic loads were applied with a mechanical oscillator and a speed controlled D.C. motor mounted onto the wall so as to give a dynamic load at the same level as the static load. Fig. 1 shows the test setup. A static load was first applied and values of deflections noted when they became constant. Dynamic load of different magnitudes were then applied by changing the angle of setting of eccentric masses of the oscillator as well as the frequency. For each combination, the residual deflection after 30 seconds of dynamic load application over and above that due to static load applied was measured. Different combinations of static load and dynamic load were

chosen and the observations repeated.

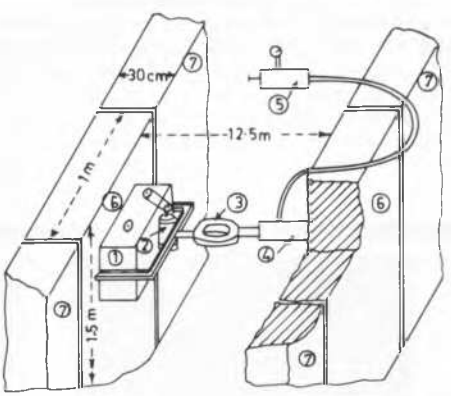

1-MECHANICAL OSCILLATOR
2-ELECTRIC MOTOR
3-DYNAMOMETER
4-HYDRAULIC JACK
5-REMOTE CONTROL
6-TEST WALL
7-SIDE WALL

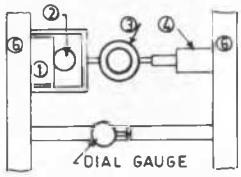

Fig. 1 Set-up for passive pressure test

From the test data the lateral deflections corresponding to static loads and total deflection (static and additional dynamic) due to total lateral load (static and dynamic) were computed using the incremental approach and are shown in Fig. 2 by firm line and points respectively (numbers indicate frequency of dynamic load). Plots obtained at both locations were similar. It is also observed that points corresponding to dynamic loads lie in a very narrow band indicating thereby that strength of cohesionless soil at this site is only slightly affected by dynamic loads. Failure strength determined by (i) the intersection of tangents to the two straight portions of the envelopes of the points and (ii) intersection of tangents to the full line curve showed that the difference in the ultimate values is very small (Prakash et al, 1973).

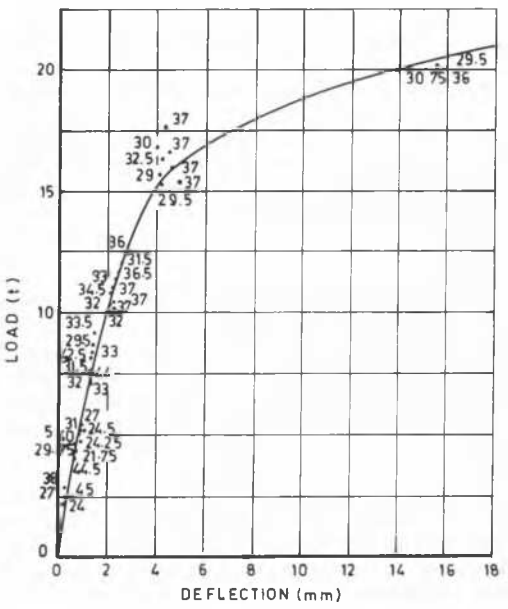

Fig. 2 Load displacement plot for passive pressure test

Observation on behaviour of material behind the retaining walls indicated general heaving of the ground and cracks radiating from the ground but no well-defined rupture surface was observed even at the largest displacements applied. Treating the problem as three dimensional and angle of wall friction, δ, as $\tan^{-1}(0.6 \tan 2/3\ \phi)$, where ϕ is the angle of internal friction for the material, the values of ϕ were computed from the observed passive pressures and were of the order of 33.15° to 35.5° which are close to those observed in static tests conducted at the site using large size shear box (cross-sectional area of sample 1.5m x 1.5m).

CONCLUSIONS

1. The angle of internal friction of cohesionless soils is the same under static and dynamic loading.
2. Special testing techniques have occasionally to be used to develop confidence with a geotechnical engineer by establishing validity of certain assumptions usually made.

REFERENCE

Prakash, Shamsher et al (1973), "final Report on Soil Investigations for Cement Factory at Rajban (H.P.)," A report on Soil Investigations Carried out by Department of Civil Engineering and School of Research and Training in Earthquake Engineering, University of Roorkee, Roorkee (U.P.) India.

Chairman Seed

Now I would like to ask Professor Hansbo to conclude this part of the program with his comments on that discussion or related matters.

Panelist: S. Hansbo

In an article presented in Vol. 2 of the Proceedings of this conference I showed how dynamic ground pressure vs settlement loops can be used to predict the ground pressure vs settlement curve obtained in static loading of a shallow footing. I would like to explain here how dynamic pre-loading of a bored end-supported pile can be used for the twofold purpose of improving its bearing capacity and predicting its settlement due to "static" loading. It is presumed that the pile tip is not resting on clay or fine-grained silt.

For the study of the dynamic response, a prefabricated pile tip is placed on the bottom

of the excavation, Fig. 1. On the pile tip is placed a watertight measuring device of steel, instrumented with strain gauges and an accelerometer. The pile tip and the measuring unit are called here "the foot". A steel column, built up of jointed pipes, Fig. 2, is placed on top of the foot. On the top of the steel column, a guide casing is placed and in this guide casing the hammer is dropped. The blow of the hammer is damped, either by a hard rubber cushion or by an air-water damping system. Air-water has proved to give better damping than rubber. A rod from the ground surface is fixed to the pile tip and connected to an inductive linear variable displacement transducer (LVDT).

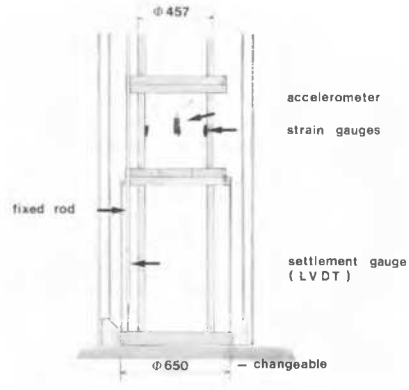

Fig. 1 The "foot". Pile tip and measuring unit of steel instrumented with accelerometer and strain gauges. "Fixed rod" connected to an inductive displacement transducer (LVDT).

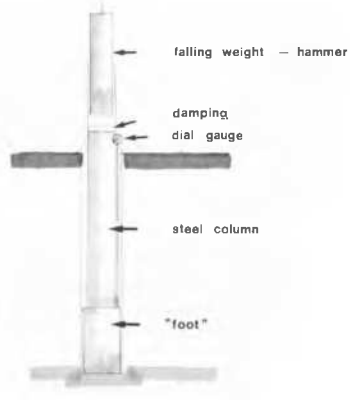

Fig. 2 Set-up for dynamic preloading. Steel column consisting of jointed pipes with an outer diameter of 457 mm and a wall thickness of 40 mm. Weight of hammer = 3800 kg.

After that these arrangements have been made, the pile tip is subjected to several blows of the hammer, thereby causing dynamic preloading of the subsoil beneath the tip, Fig. 3. The steel stress σ and the deceleration $-d^2s/dt^2$ of the measuring unit are studied (steel stress variation in bottom of figure, deceleration in top). Now, assuming that the wave velocity is infinite in steel in

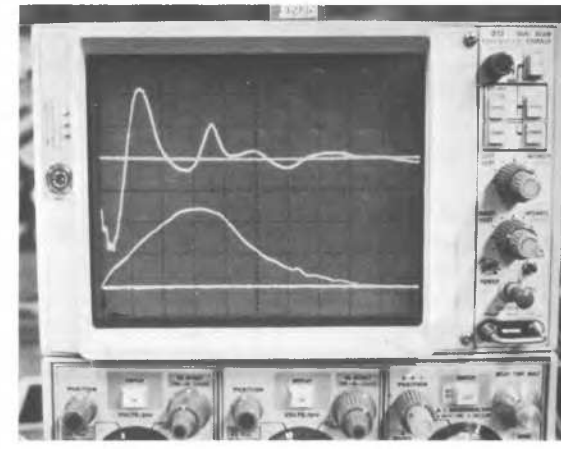

Fig. 3 Steel stress and deceleration of measuring unit observed by means of oscillograph (deceleration in top).

comparison with that in the subsoil, Newton's 2nd law can be used for the determination of the variation of contact stress with time during the blow of the hammer.
We have

$$p-\sigma = -(m/A)\,d^2s/dt^2$$

where

m is the mass of the foot below the gauge level
A is the base area of the pile tip

From the deceleration, the vertical displacement s of the pile tip vs. time, during the blow, can be found by double integration and the result of this can be checked against the LVDT signals. In this way we find the relation between the contact pressure, pile tip/subsoil, and the settlement of the tip during the blow.

To study how dynamic preloading affects the bearing capacity and to see if the dynamic response can be used to predict the settlement in static loading, several full-scale and small-scale tests have been made as part of a Doctoral work by Bo Berggren at Chalmers University of Technology, Sweden.

I would like to present a few typical results obtained in the full-scale tests. The tests refer to piles founded below water in till. The diameter of the pile tip was 0.65m, i.e. the same diameter as in Fig. 1. Fig. 4 shows a comparison of the load vs. settlement curve obtained before and after dynamic preloading. It is quite obvious that the subsoil below the pile tip has been considerably improved

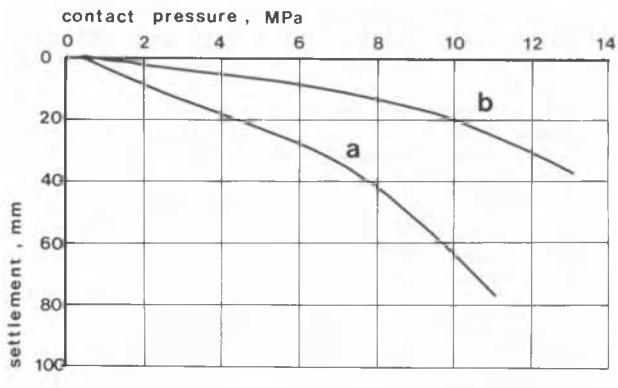

Fig. 4 Load vs. settlement curves obtained in static loading before (curve a) and after (curve b) dynamic preloading.

by the dynamic treatment.

Fig. 5 shows how long the dynamic action had to continue - in other words, the dynamic input required - in our case before a dynamic overconsolidation ratio, as I would call it, of any significance was obtained. Obviously, the smaller the ratio of remaining plastic settlement to total settlement during the blows, the better the result.

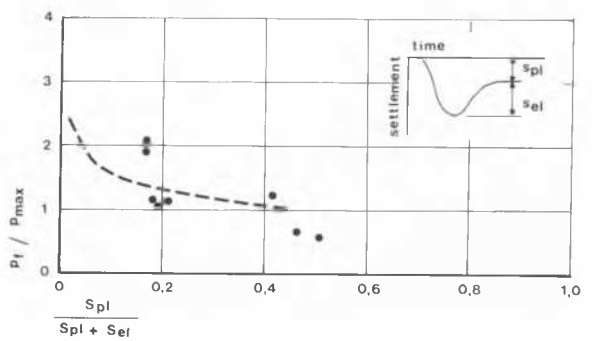

Fig. 5 Ratio of bearing capacity in static loading p_f to maximum pressure p_{max} in dynamic preloading vs. ratio of remaining plastic settlement s_{pl} to maximum settlement $s_{pl} + s_{el}$ obtained by the final blow of the hammer in dynamic preloading.

In Fig. 6 the dynamic ground pressure vs settlement loop is compared with the ground pressure vs settlement curve obtained in a static loading test carried out immediately after the dynamic preloading. In the static test, the load was applied in 10 equal steps up to estimated failure load, corresponding to 0.5 to 1.5 MPa stress increase per step.

In each step the load was kept constant for 16 min. In the diagram, curve (b) includes the accumulated 16 min creep settlement obtained in the successive load steps while curve (c) excludes these creep settlements. We find that the deviation of the static response from the dynamic, indicated by curves (b) and (a), is almost completely eliminated if corrections are made with due regard to the creep taking place during the loading process, as indicated by curve (c). If such a correction is not made, the difference in inclination of the static and dynamic load vs settlement curves will be larger the more fine-grained the subsoil beneath the pile tip.

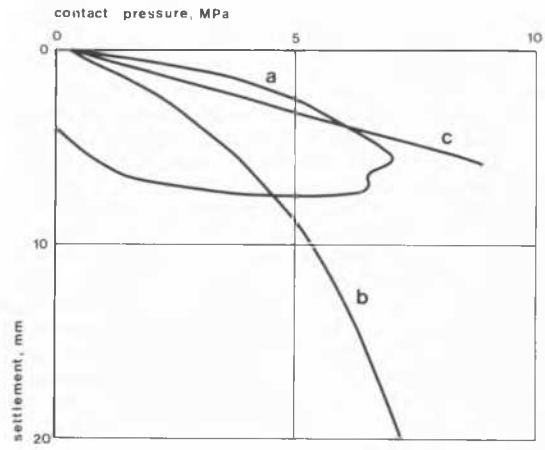

Fig. 6 Comparison of pressure vs. settlement curves obtained in a) dynamic preloading, last blow of the hammer, b) static loading, including creep during time of load step (16 min. duration), c) static loading, excluding, creep.

The given examples demonstrate that there is a good possibility of replacing the extremely expensive full-scale static loading tests, previously considered necessary for predicting the static behaviour, by comparatively inexpensive dynamic tests and of gaining, at the same time, a better pile both with respect to settlement and with respect to failure.

(Intermission)

Chairman Seed

I am now going to invite Professor Ishihara to be the first speaker in the floor discussion this morning.

K. Ishihara (Japan)

Investigation of Liquefied Sites in Niigata, Japan

Using a large diameter sampler developed recently (Ishihara and Silver, 1977), undisturbed lumps of loose sands (20cm in diameter and 80cm long) were secured from bored holes drilled at two sites in Niigata where liquefaction of the ground developed extensively at the time of the 1964 Niigata earthquake. After the big lump samples have been completely drained, the core barrel consisting of two halves was dismantled and the intact sand surface exposed. Small brass tubes 5cm in diameter and 10cm long were then inserted into the big sand block to provide small specimens for cyclic triaxial testing. The specimens were frozen in the field and carried to the laboratory. Cyclic triaxial shear tests were performed under the confining pressures corresponding to the in-situ overburden pressure. The cyclic stress ratio, $\sigma_{d\ell}/(2\sigma_o')$, required to cause initial liquefaction 5% and 10% double amplitude axial strains were determined for each lump sample taken from different depths, where $\sigma_{d\ell}$ is the amplitude of cyclic stress and σ_o' is the initial confining pressure. The location of this test site is indicated in the map shown in Fig. 1. Following the 1964 event, damage surveys reported severe evidence of liquefaction at this location in the form of sand volcanoes and resulting inundation all over the ground surface. The area had been in the flood plain of the river. Up to about 1955, the area was approximately 4m lower and was the bed of the Shinano river, sometimes having been dried in dry seasons. Subsequently, the area was reclaimed in 1955 by dumping sand through water and then by placing borrow sands.

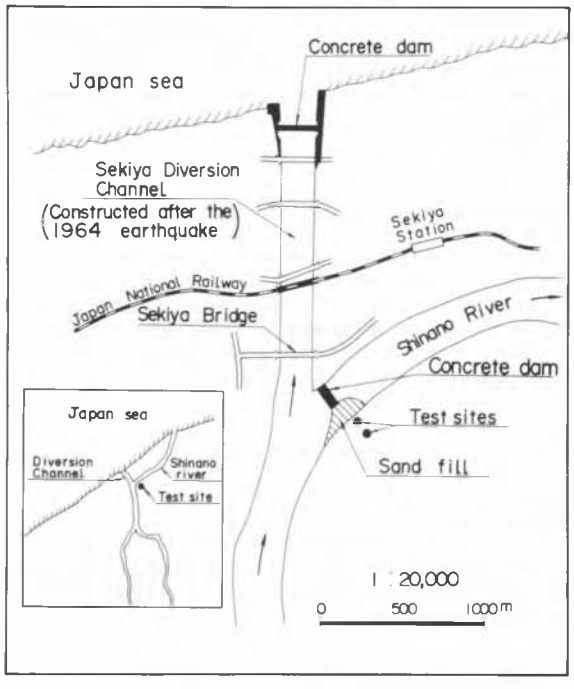

Fig. 1 Location map of the test site in Niigata

Soil conditions there are shown in Fig. 2 which plots soil type, soil formation, and N-values obtained from standard penetration tests. Thus, the soil deposition at the site

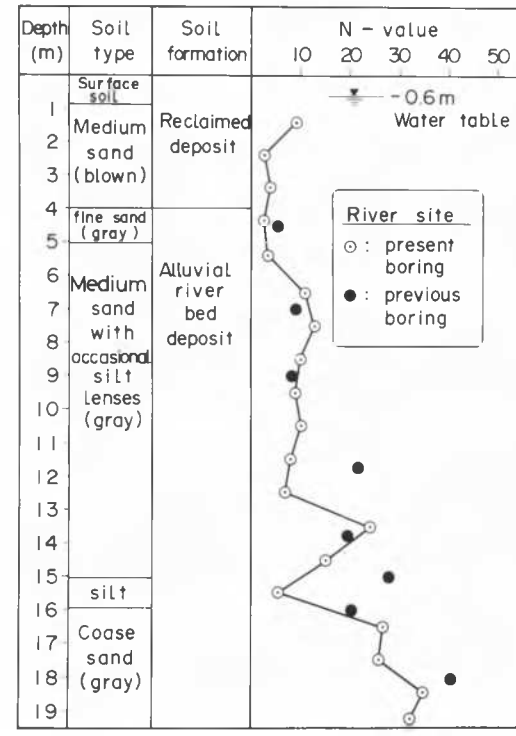

Fig. 2 Soil profile at a site near the Shinano river in the city of Niigata

was 1) uncompacted fill dumped in air in the top 1m; 2) undensified fine sand dumped through water between a depth of 1 to 3m; 3) overconsolidated sand layer of the original river bed from 3 to 5m and 4) fluvial river deposits below 5m consisting of medium sand with occasional silt lenses. At depth, there are some silt layers underlain by a uniform coarse sand. Standard penetration test values show that the blow counts at the site are low and generally do not exceed 15 to a depth of about 13m.

Each of the small specimens obtained from the large diameter sand samples was tested to determine in-situ relative density, grain size characteristics and cyclic triaxial strength. Grain size distribution curves for soils from various depths indicate that predominantly the soil consists of medium sand with mean grain size values between 0.35mm and 0.55mm, except at a depth of 4.5m where a fine sand was found and at a depth of 9.5m where a coarse sand was encountered.

Relative density values at each depth are demonstrated in Fig. 3 where it is noted that in the reclaimed sand, relative density values ranged between 20% and 50% with a general increase in relative density with increasing depth beginning at a depth of 5m.

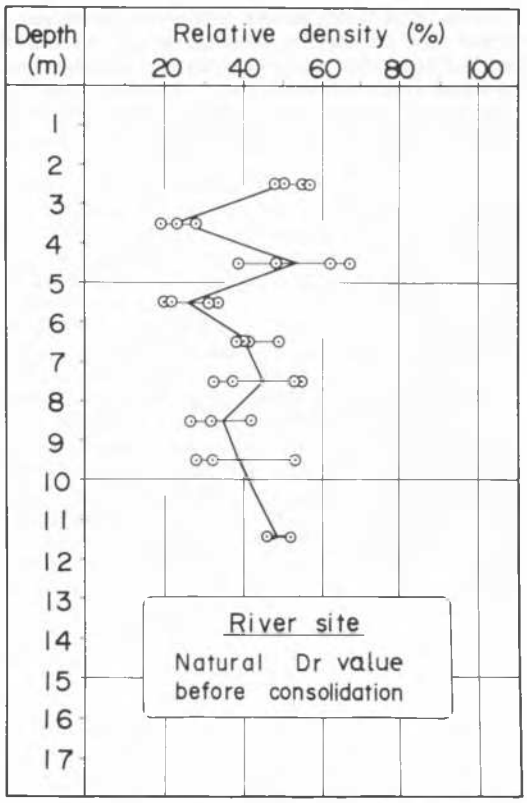

Fig. 3 Insitu void ratio versus depth

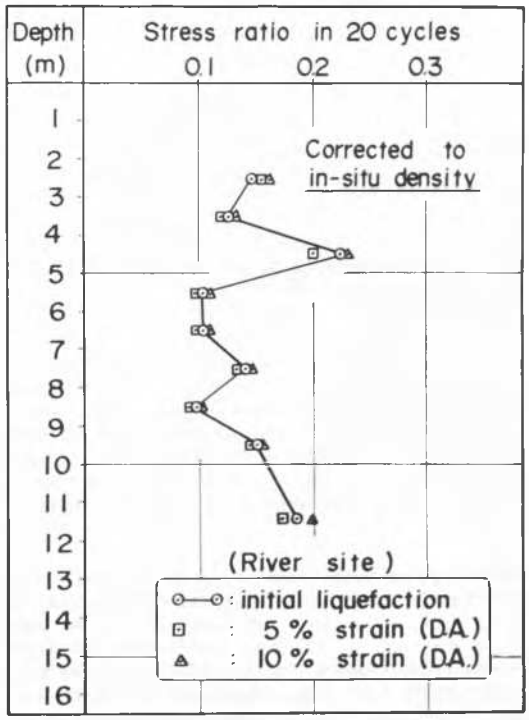

Fig. 4 Cyclic stress ratio versus number of cycles to initial liquefaction, 5% and 10% double amplitude strain

It is useful to show the cyclic triaxial strengths of undisturbed soil specimens at the test site as a function of depth at their estimated in-situ relative density values. This is done in Fig. 4 which plots the cyclic stress ratio necessary to cause failure (initial liquefaction, 5% and 10% double amplitude) in 20 cycles versus the depth. It may be seen that in the reclaimed zone, down to a depth of 4m, the cyclic stress ratio necessary to cause failure in cyclic triaxial strength tests is on the order of 0.15 and that in the transition zone between the reclaimed layer and the natural river bed deposit the cyclic stress ratio required to cause failure in 20 cycles increases to 0.22. In the natural deposit, the cyclic stress ratio is on the order of 0.1 at shallow depths, increasing uniformly to a value of 0.2 with greater depth.

Many civil engineers and geologists believe that there exists very slow movement of the ground water along the Shinano river in the area of the city of Niigata. There are good reasons to believe that the ground water flows slowly through a layer located at depths approximately between 5m and 10m. As a matter of fact, it was extremely difficult to secure a complete block sample from these depths during the operation of large diameter sampling. Scouring and piping developed extensively through a narrow opening left by incomplete closing of two sets of core catcher nets when the larger diameter sampler was lifted from bore holes. Fresh water was observed at this instance washing out the sand near the core catcher. The existence of the ground water flow may account for the formation of an extremely loose deposit below the depth of about 4.5m.

REFERENCE

Ishihara, K. and Silver, M.L. (1977)„ "Large Diameter Sand Sampling to Provide Specimens for Liquefaction Testing," Soil Sampling, 9th International Conference on Soil Mechanics and Foundation Engineering, Tokyo, pp. 1-6.

Chairman Seed

Professor Jessberger.

H.L. Jessberger and Mr. H.J. Gödecke (F.R.G.)

Theoretical Concept of Saturation of Cohesive Soils by Dynamic Consolidation

SYNOPSIS The phenomenon of Dynamic Consolidation, a compaction method which has appeared in soil mechanics since nearly seventies, has been originally explained on the base of thixotropy. Since 1975 the Ruhr-University in Bochum has devoted a systematic effort to describe this phenomenon within the framework of fundamental laws of soil mechanics. In the following will be presented an analysis of stresses measured in a test of Dynamic Consolidation as described by GÖDECKE (1976).

INTRODUCTION

With the Dynamic Consolidation method very high impulse loads are applied to cohesive, mostly saturated soils. Features observed during this process are presented on Fig. 1.

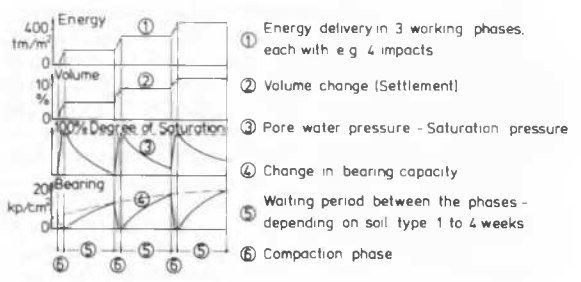

Fig. 1 Effect of impact energy on soil during three compaction phases (after Menard)

It is understood that the bearing capacity was determined using the Menard's Pressiometer. The state of full saturation corresponded to a level of pore pressure, which do not increase any during further impulse loading.

LABORATORY TESTS, MEASURED RESULTS AND THEIR ANALYSIS

To investigate its features the process of Dynamic Consolidation was simulated in laboratory. A steel cylinder, 15cm in diameter and 20cm high was used. The impulse loading was modelled by a relatively small mass falling at the center of the soil specimen.

Illustrations of the test results are presented in Fig. 2. Totally 14 loading impulses were applied in this test. After this number of impulses the pore pressure reached a limiting level resisting any further increase. The saturation is defined as the ratio of $\Delta u/\sigma'_z$.

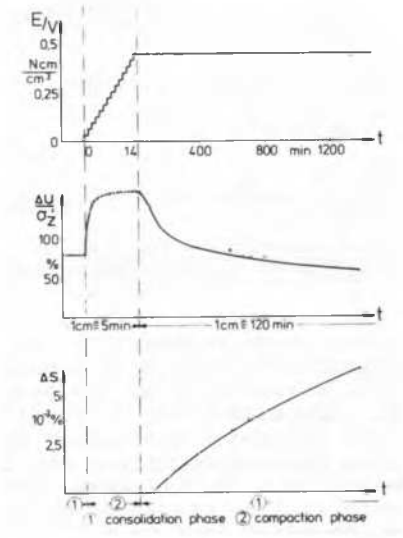

Fig. 2 Laboratory test of dynamic consolidation

Here Δu is the increment of pore pressure above the hydrostatic pressure. σ'_z is the nominal effective stress, which acted initially in the vertical direction. It will be used as a constant reference value and normalizing factor throughout the pore pressure history.

The loading phase is followed by the dissipation phase, during which the process of consolidation is registered. At the same time a volume change takes place. This is because during the dissipation phase a change of stresses within the soil specimen, even without change in external load must take place. Using another system of measuring devices in addition the total stresses were recorded after every impulse load application. Together with the measured pore pressures this provides the possibility to calculate effective stresses. The results of such calculations are presented in Fig. 3. Before the impulse loading application the effective stress ellipse is stretched vertically. Every single impulse of the dynamic loading decreases the effective stresses in vertical direction.

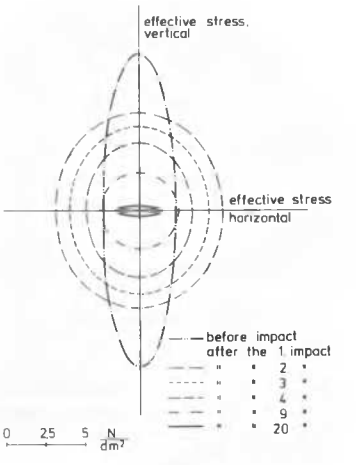

Fig. 3 Measurements of stress during impulse loading

The stress ellipse after the 20th impulse is given by the full line in Fig. 3. The horizontal effective stresses, when compared with the initial condition show an increase first followed by a reduction later. Also, after the 20th impulse there is a complete 90-degree rotation in the direction of principal stresses.

To investigate the conditions of failure the Mohr's circle presentation of stresses will be used. It is given on Fig. 4. The Mohr's envelope for $\phi' = 37°$ has been determined from triaxial tests on unconsolidated samples. The same soil was then tested in dynamic impulse loading. With the application of the impulse loads the effective vertical stress of 20.0 N/dm^2 has decreased to 4% of its initial value. The corresponding reduction in the effective horizontal stress is only

60.4%, so that the rotation of principal stresses has taken place. Should the effective horizontal stress in the saturated sample be increased rather than decreased, then the value of 2.9 N/dm^2 would have to increase. Thus the diameter of the Mohr's

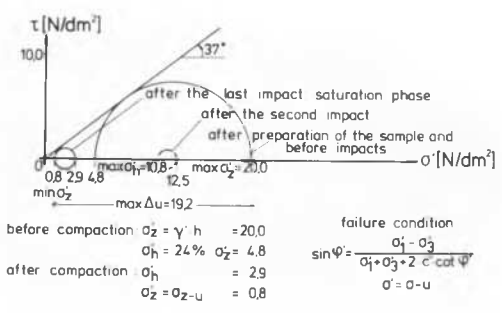

Fig. 4 Mohr's circles after impulse loading

circle would have to extend to the right. This is, of course, not possible as the circle cannot extend above the strength envelope. Exactly this is what happens with the Menard's Pressiometer, when it is used in-situ on saturated soils and a horizontal stress is applied. The test reaches a failure condition and larger deformations are obtained by smaller stresses, resulting in reduced stiffness.

CONCLUSION

Analysed above is a soil mechanics phenomenon, appearing during Dynamic Consolidation. Using data from laboratory measurements there appears to be a possibility to explain this phenomenon within the framework of fundamental laws of classical soil mechanics. The analysis of stresses in the Mohr's diagram provides indications about the conditions of failure during the dynamic saturation process.

REFERENCES

Bobylev, L.M. (1963), "Raspredelenie naprazenij deformacij pletnofte v grunte pri uplotnenij nsaytej trambyjuscini plitom," Osnovanija Fundamenty i Mechanika Gruntov, Vol. 5, No. 6, pp. 1-4.

Gödecke, H.J. (1976), "Bodenverflüssigende Impulslasten auf bindigem Boden," Deutsche Baugrundtagung Nürnberg.

Jessberger, H.L. (1977), "Beitrag zu den theoretischen Grundlagen der dynamischen Intensivverdichtung," Techn. Akademie Wuppertal.

Menard, L. and Broise, Y. (1975), "Theoretical and practical aspects of dynamic consolidation," Geotechnique 25, No. 1, pp. 1-18.

Chairman Seed

And now I would like to invite Dr. Haupt to present his discussion. This involves a movie film, and I think you might find it of considerable interest.

W. Haupt (F.R.G.)

The isolation of buildings against elastic waves, propagating in the ground, is becoming more and more important. An investigation by Finite-Element-method has been performed on the screening effect of stiff, solid obstacles within the homogeneous half-space against steady-state harmonic surface-waves. Some results are reported in a contribution to the proceedings of this conference. In connection with the above mentioned calculations a computer movie has been prepared, showing some cases of the behaviour of surface-waves in the vicinitv of a solid obstacle by the cyclic deformation of the FE-grid. I wish to present this movie here.

The investigation deals with a plane strain problem and the material is chosen to be linear visco-elastic. All geometrical parameters are normalized on the Rayleigh-wave length. The ratio of the shear moduli was $G_w/G_h = 34.3$ and that of the densities is chosen to be $\rho_w/\rho_h = 1.37$, where the subscript w indicates the obstacle material and the subscript h the half-space material. The Poisson's ratios are equal. From these material parameters results a ratio of wave velocities $v_w/v_h = 5.0$. Thus, the obstacle material approximately represents concrete, when compared with natural soil.

The upper boundary of the FE-grid is the free surface of the half-space. At the lower boundary a full-space condition ("dashpot" - BC) is used. At the right and the left vertical boundaries of the grid conditions are applied, which perfectly replace the adjacent infinite quarter-spaces (EM-BC).

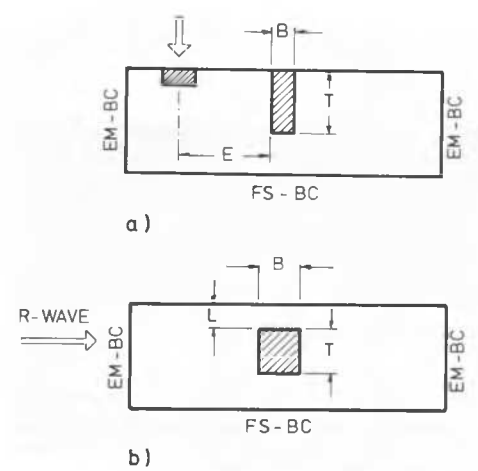

Fig. 1 FE-system a) near-field isolation, b) far-field isolation

First the case of near-field isolation is considered. The wave source is a strip foundation at the surface, being subjected to a harmonical vertical force (see Fig. 1a).

In the first case there is no obstacle within the half-space that means there is only the oscillating foundation (see Fig. 2). The typical deformation field can be observed: Below and to the side of the foundation body-waves are spreading out into the half-space. At the surface the Rayleigh-wave is dominant even at short distance from the foundation.

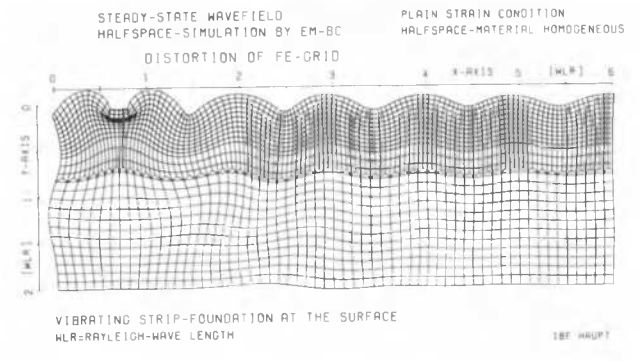

Fig. 2 Vibrating strip foundation without obstacle

The next case, which is presented in Fig. 3, shows the screening of the waves by an obstacle, which can be considered as a concrete core wall. Its depth is 1.5 times the Rayleigh-wave length. At the surface almost a standing wave is generated, due to the reflection of the waves at the wall. Within the half-space the reflection of the incoming waves can be observed directly.

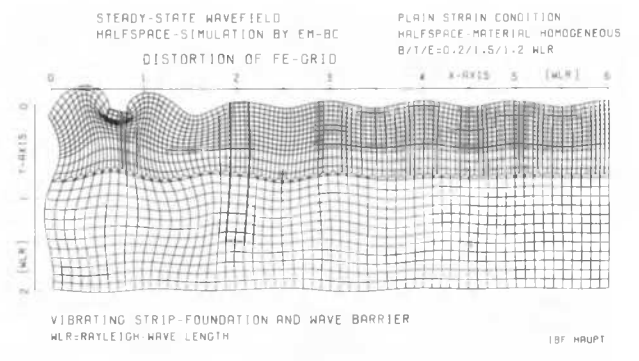

Fig. 3 Near-field isolation, E = 1.2 WLR

In the Fig. 4 the case of a thin wall near to the foundation is presented. This is an approximation of a sheet pile wall, although that would even be thinner. This wall follows quite well the motion of the surrounding half-space. Therefore the screening effect of this sheet pile wall is very small.

Some cases of obstacles in the far-field of a wave source are presented in the following.

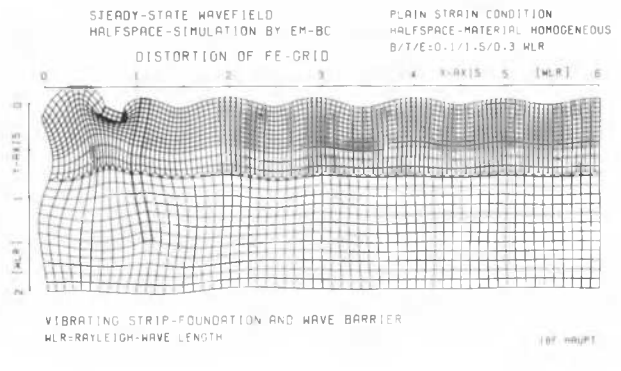

Fig. 4 Near-field isolation, E = 0.3 WLR

The system is represented in Fig. 1b. The Rayleigh-wave in its theoretical mode penetrates from the left into the FE-field.

Fig. 5 shows the distortion of this Rayleigh-wave field by a wall-shaped obstacle with the dimensions of 0.2 x 1.0 Rayleigh-wave lengths. At the surface a partial reflection of the incoming waves can be observed. In the lower part of the half-space body-waves are spreading out from the end of the obstacle similar to the case of the oscillating foundation.

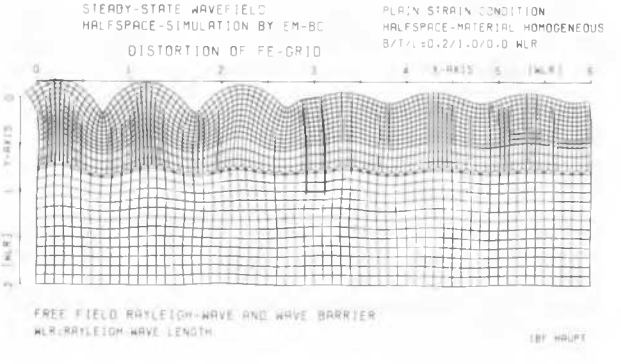

Fig. 5 Far-field isolation, deep obstacle

Thus, the obstacle acts like a new wave-source within the half-space.

In the case of a wide, shallow obstacle, which can be seen in the Fig. 6, body-waves also occur. They are generated at the hori-

zontal interface between the obstacle and the half-space. Due to interference phenomena the screening effect of this obstacle is as good as that of the foregoing one.

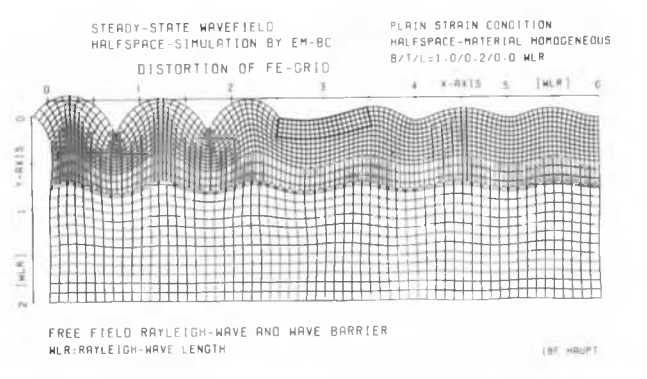

Fig. 6 Far-field isolation, shallow obstacle

Finally a square bloc at the depth of 0.3 Rayleigh-wave lengths below the surface is considered (Fig. 7). Although the obstacle

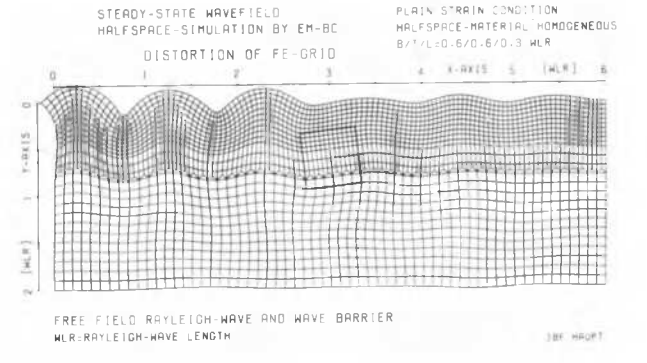

Fig. 7 Far-field isolation, obstacle below the surface

does not reach up to the surface the reflections are strong and also strong body waves are generated in the lower part of the half-space. This obstacle has a very good screening effect.

The moving picture film is an appropriate way of regarding dynamic problems, because it includes the dependency of the displacements both on time as well as on the space variables. The visualization of the displacements and strains below the surface and around the obstacle provides a better understanding of the wave propagation processes within the half-space and enables the engineer to arrive at an effective design of screening measures.

Chairman Seed

Thank you very much. Monsieur Le Tirant.

P. Le Tirant (France)

Action de la Houle sur les Fondations de Plates-Formes Marines a Embase Poids

(Effect of Wave on Offshore Foundations Gravity Platforms)

INTRODUCTION

Les lois de similitude applicables aux modèles de fondations marines et les premiers résultats ont fait l'objet de la communication 4/19, Vol. 2, p. 277 des Comptes Rendus du IXè Congrès International de Mécanique des Sols (Tokyo). Cette intervention complète la communication précédente en donnant les résultats essentiels du comportement des fondations de plates-formes à embase poids sous l'action de la houle (Fig. 1). Ces résultats sont déduits de plusieurs séries d'essais de simulation par centrifugation.

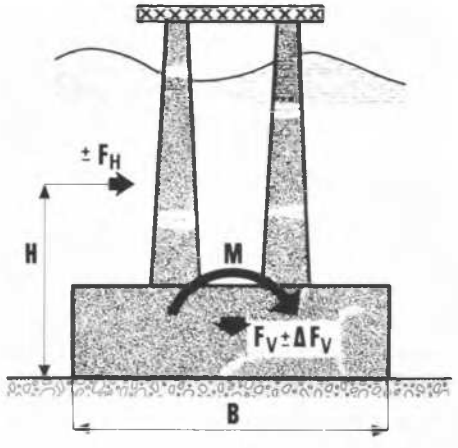

Fig. 1 Forces s'exerçant sur une plate-forme à embase poids

1. PRINCIPE DES SIMULATIONS

Les simulations par centrifugation réalisent l'egalité des contraintes en tous points homologues du modèle et de la fondation réelle.

La fondation est soumise à des basculements et poinçonnements cycliques simulant l'action de la houle.

Chaque essai correspond à la simulation d'une tempête en Mer du Nord:
- l'amplitude crête à crête de la houle simulée croît jusqu'à 30 mètres environ,
- la période croît de 5 à 15 secondes,
- le nombre de cycles est de l'ordre de 1 000.

Le modèle est réalisé à l'échelle 1/100 (Fig. 2). La centrifugeuse permet d'atteindre une accélération de 100.g en fonctionnement continu. Pour la description de l'appareillage et du modèle utilisé, on se reportera

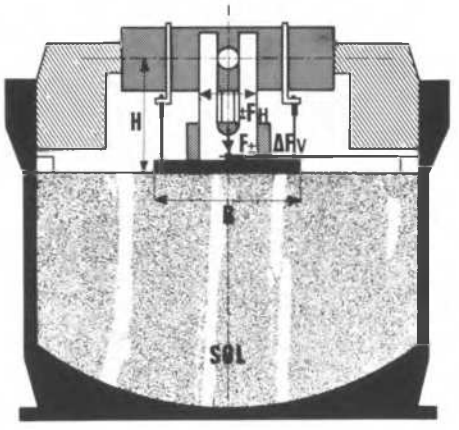

Fig. 2 Schéma du modèle réduit

à la communication précitée. Les résultats obtenus sur un modèle simulant une fondation de diamètre B = 30m environ sont extrapolés à une fondation de base (côté ou diamètre) B = 100m.

2. SOL DE FONDATION

Pour les premières séries d'essais, le sol de fondation était constitué d'un sable fin (sable de Fontainebleau), de granulométrie comparable aux sables rencontrés sur plusieurs sites de Mer du Nord ($D_{50} \simeq$ 100 à 150µ). La densité relative était comprise entre 30% et 60% suivant les séries d'essais.

3. RESULTATS OBTENUS

Les résultats obtenus concernent:
- d'une part, les déplacements horizontaux et verticaux de la fondation,
- d'autre part, l'évolution de la pression interstitielle dans le sable de fondation.

3.1. Déplacements de la fondation

Les variations du déplacement horizontal cyclique 2 d_h et du basculement cyclique 2 d_V de la fondation d'une structure de base B = 100 mètres en fonction du rapport F_H/F_V, sont représentées sur les figures 1 et 2, où F_V poids apparent (immergé) de la plate-forme, voisin de 2,4 GN (240 000 tonnes), F_H effort horizontal dû à l'action de la houle.

Pour une houle centenaire de 30 mètres, correspondant à un effort horizontal F_H = 0,8 GN (80 000 tonnes), on observe:
- un basculement cyclique d'une quinzaine de centimètres,
- un déplacement horizontal cyclique d'une dizaine de centimètres.

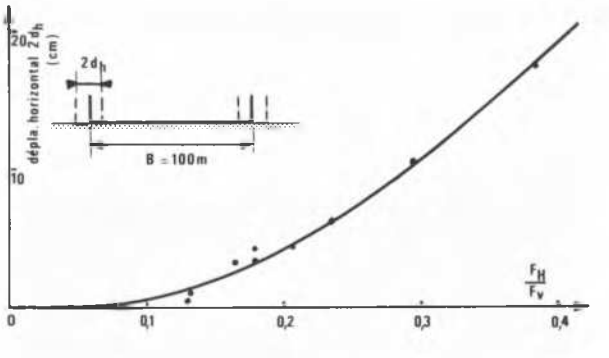

Fig. 3 Déplacement cyclique horizontal d'une structure B = 100 mètres en fonction du rapport F_H / F_V

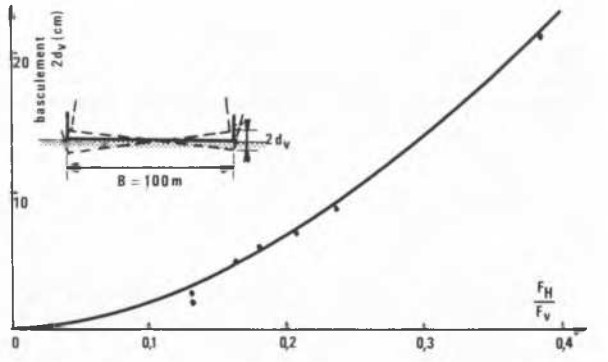

Fig. 4 Basculement cyclique d'une structure B = 100 mètres en fonction du rapport F_H / F_V

Le ripage (déplacement horizontal permanent) de la fondation et le tassement du sol demeurent relativement peu importants et ne semblent pas mettre en péril la stabilité de la structure reposant sur le sable.

3.2. Pression interstitielle dans le sol de fondation

Les mesures effectuées en différents niveaux sous la fondation n'attestent pas d'accroissement significatif de la pression interstitielle dans le sable avec la répétition des chargements. Ces résultats s'accordent bien avec certaines mesures effectuées sous des fondations de structures réelles reposant sur du sable (ou des alternances sable/argile) montrant un accroissement peu important de la pression interstitielle au cours d'une tempête.

CONCLUSIONS

Les différentes mesures effectuées sont bien

reproductibles et permettent de se faire une idée globale du comportement de la fondation.

Dans le cas de structures gravitaires reposant sur du sable et soumises à une houle centenaire de 30 mètres, on peut prévoir:
- des déplacements décimétriques de la fondation,
- des variations relativement faibles de la pression interstitielle sans risque de réduction significative des contraintes effectives dans le sol.

Chairman Seed

Thank you. Professor Dawson.

A. Dawson (Mexico)

Soil Conditions for the Liquefaction Case History, Chiapas

In volume 2 of the proceedings of this conference there is a paper which presents a number of field observations on the liquefaction which occured during two small magnitude earthquakes in Chiapas, Mexico (Flores Berrones and Dawson, 1977). This discussion presents some more recently obtained information on the subsoil conditions in the areas where liquefaction was observed.

Borings were performed to define the stratigraphy, classification and standard penetration resistance in the areas where liquefaction was observed. Wash borings with split tube samplers were used in the exploration program, and the penetration data thus obtained were augmented by continuously driven cone penetration resistances performed next to each borehole. In most areas there was a surficial cohesive layer of variable composition (Fig. 1) which is underlain by alluvial medium uniform sands such as was shown

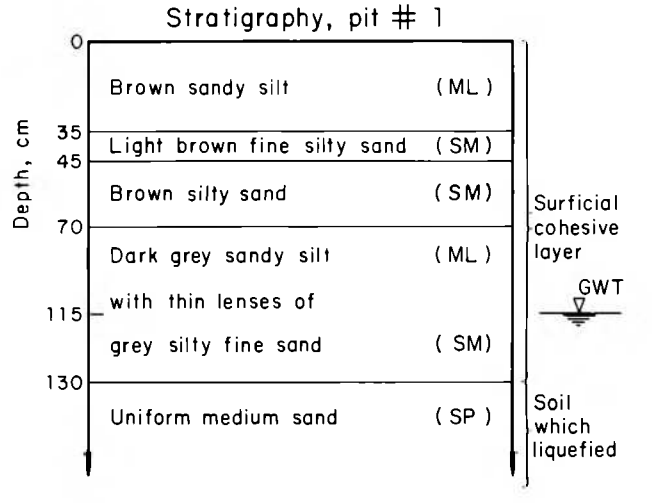

Fig. 1 Typical near surface soil profile where liquefaction was observed

in Fig. 6 of the paper in Vol. 2. In some local areas there were lenses of silty fine sand in the cohesive surface layer which probably liquefied, and the two grain size curves of fine sand presented in Fig. 5 of the original paper are representative of those materials. Trenches were dug in many places where liquefaction had been observed a year earlier, and the sand filled cracks in the surface cohesive layer were located and observed. The grain size data in Fig. 2 come from the material in those cracks.

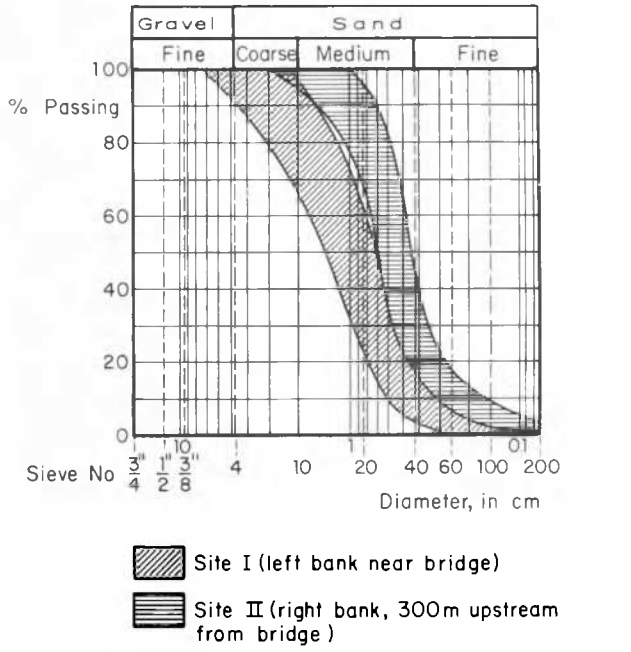

Fig. 2 Grain size distributions of sands which liquefied and were trapped in fissures

The uniform medium sands beneath the cohesive surface layer are the ones in which the most important liquefaction occurred. Undoubtedly the impeded upward drainage caused by the cohesive surface layer was a contributing factor in producing liquefaction. No layers of materials significantly different from those indicated in Fig. 2 were observed within the main body of the alluvial sands.

In all borings there was a rapid increase in penetration resistance with depth. The range of penetration resistances measured in the sands is presented in Fig. 3 as a function of overburden pressure; and the Gibbs and Holtz correlation for relative density is provided for reference. No undisturbed samples of the sands could be taken with the equipment used in exploration and consequently the actual values of relative density are unknown. The correlation used in Fig. 3 is less reliable at low overburden pressures and there is some evidence that it may be somewhat conservative in the region of interest (Zolkov, Wiseman; 1965). In any case it is clear that the sands which liquefied are those just below the surficial cohesive

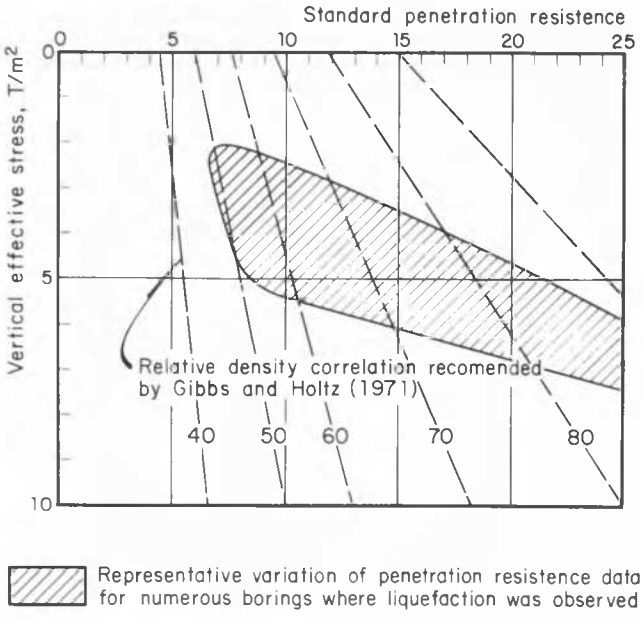

Fig. 3 Penetration resistence of sands where liquefaction was observed

layer and probably above a depth of 3 to 4 meters where their correlated relative density is between 50 and 65%. The envelope shown in Fig. 3 includes about 90% of the penetration resistances measured at 8 boring locations so the lower bound of the zone, at 50% correlated relative density is probably a bit lower than the average condition where liquefaction was observed.

REFERENCES

1. Flores-Berrones, A. and Dawson, A. (1977), "A Liquefaction Case History in Chiapas, Mexico," Proceedings of the 9th ICSMFE, Tokyo, Vol 2, p. 237.

2. Dawson A., Flores-Berrones A., (1976), "Estudio de licuación de arenas en Chiapas, Parte 1. Evaluación de las observaciones preliminares de las manifestaciones de licuación," Proy 5182, Instituto de Ingeniería, UNAM.

3. Dawson A., and Arenas A. (1976), "Estudio de licuación de arenas en Chiapas, Parte 2. Resultados principales de las exploraciones geotécnicas en las áreas de licuación," Proy 5182, Instituto de Ingeniería UNAM.

4. Gibbs, H. (1971) "Standard penetration test for sand denseness," Proc 4th Pan American Conference on Soil Mechanics and Foundation Engineering, Vol. II, p. 37-44.

5. Zolkov, E. Wiseman G., (1965), "Engineering properties of dune and beach sands and the influence of stress history," Proc 6th ICSMFE, Montreal, Vol. I, p. 134-138.

Chairman Seed

It seems to be the task of the Session Chairman to draw these meetings to an end, usually at a point where the discussion has reached a peak of interest and much worthwhile information remains to be presented.

However end they must, and in the final ten minutes the Chairman is asked to offer his comments on the proceedings of the Session and the State-of-the-Art. I hope you were as impressed as I have been with the progress and new developments in the field of soil dynamics related to us by Professor Yoshimi and his co-reporters, by our Panel members and by members of our Society who have had the opportunity to speak this morning. Our knowledge of dynamic stress-strain relationships, soil response to cyclic loads including such problems as earthquake induced or storm induced liquefaction and embankment stability, earth retaining structures, the dynamic behaviour of bases and foundations, and the analytical treatment of soil-structure interaction effects is clearly well advanced; and it is my personal impression that our analytical capabilities have developed so rapidly that they tend to be limited more by our ability to determine the correct soil parameters to incorporate in them, than by limitations of the analytical procedures themselves. Although much has been accomplished we have still much to learn concerning soil behaviour and soil properties under dynamic loadings in order to establish the correct parameters to incorporate in our theories.

For example, it seems that we still lack the capability to characterize fully the in-situ properties of a body of cohesionless soil, and while in-situ testing techniques are making rapid headway to help us in this problem area, our inability to extract and handle undisturbed samples of sand is a severe limitation to progress in predicting and evaluating probable field performance.

Probably the greatest limitation of all, however, is the great lack of field case histories by which we can check the applicability of our design and analysis procedures for predicting performance in the real world. Nowhere is this more difficult to accomplish than in the field of earthquake soil dynamics. It is of comparatively little benefit to know that a particular slope failed in a specific earthquake, if we do not also know the magnitude of the dynamic excitation that caused it to fail. Detailed analysis of field performance requires a knowledge of the system geometry, the significant material characteristics and the loading system which led to the observed performance. Yet so often in the earthquake field in particular, the last item is missing since there is no way of knowing where the next earthquake may occur and placing the necessary instruments to record the ground motions it produces. The rapidly advancing field of earthquake prediction may help enormously in this respect and the time may come before too long when we can specially

instrument earth structures in the knowledge that useful performance data will undoubtedly be obtained.

In the meantime we are largely forced to wait and hope; hope on the one hand that we have wisely placed instruments in locations where an earthquake will provide a good case history to check our design procedures; and hope on the other hand that no earthquake will occur to jeopardize the safety of human life and structures.

It is for this reason I believe, that we should extract from the very few case histories we do have, the maximum benefits in regard to their potential for validating or invalidating our design, analysis and testing procedures. To my mind the great significance of the slide at the Lower San Fernando Dam[1]. in 1971 lies not so much in the fact that it occurred, (although this was an important event in its own right), but that a recording instrument was available on the abutment of the dam to provide detailed information on the excitation levels existing in the area and which led to the failure. Clearly the potential use of any embankment design procedure can now be checked against this record of field performance. The detailed studies of this embankment failure including excavations to expose the failure zones, a careful determination of the configuration of the slide debris and a reconstruction of the intact pieces to better define the zone of failure, provide all engineers with the opportunity to investigate and judge the applicability of the design procedure they personally prefer.

Similarly, the records obtained at the Humboldt Bay Nuclear Power Plant in the Ferndale earthquake of 1975 provide us all with a classic case to check the applicability of analytical and design procedures for evaluating soil-structure interaction effects[2]. In this case, earthquake records were obtained in a free-field location adjacent to a deeply embedded massive structure, as well as within the structure itself, at a location where the soil properties had been evaluated prior to the event in sufficient detail to provide all engineers with the data they require to check the applicability of any procedure for evaluating soil-structure interaction effects from an initial knowledge of soil conditions, structural characteristics and dynamic excitation. This is the design problem many of us face with uncommon frequency, yet it is one of the few cases where the necessary data exists to check the applicability of any design procedures we may elect to use.

Such cases serve the same purpose in soil dynamics as detailed case studies of landslides played and continue to play in the evolution of slope stability analysis. For this reason we must be sure to use, to the full extent possible, the few cases we currently have available, and we must try to generate more, through increased field instrumentation programs; for in the final analysis, it is the ability to anticipate field performance with a sufficient degree of accuracy that is the corner-stone of engineering practice in geotechnical engineering - be it soil dynamics or soil statics.

In the soil dynamics field I believe we have travelled far, and for this we should be grateful to many workers in this important new area, but there is a long path ahead.

Let us appreciate to the full and continue the good work we have already accomplished with such enthusiasm throughout the world, but let us also be mindful of the miles still to go, in the hope that we can, in the next decade, raise the level of confidence of soil dynamics practice to that presently enjoyed in the older and more mature areas of soil mechanics and foundation engineering practice.

Above all let us be mindful of Terzaghi's concern expressed so clearly this morning by Ralph Peck, that we should not take for granted that Nature will behave in accordance with our predictions but rather take every opportunity we can to determine how Nature has actually reacted to our design and construction activities; and I might add, especially in soil dynamics, how our design and constructed facilities react to Nature's tremendous dynamic forces whether they be in the form of earthquakes, hurricanes or ocean waves as well as man-made effects such as blasts and vibrations.

I would be remiss in my duties if I did not extend our grateful appreciation to Professor Yoshimi and his co-reporters who worked so hard to prepare the State-of-the-Art report for this Session, to our Panel members for their valuable contributions this morning and to you, the audience, who have taken such an interest in the Proceedings of the Session. With that, I declare this Session closed and remind you that we meet again at 3 o'clock this afternoon in this room for the Closing Session of this Conference.
Thank you and good morning.

---

1. Seed, H. Bolton, Lee, Kenneth L., Idriss, Izzat M. and Makdisi, Faiz I. (1975) "The Slides in the San Fernando Dams During the Earthquake of February 9, 1971," Journal of the Geotechnical Engineering Division, ASCE, Vol. 101, No. GT7, Proc. Paper 11449, July, 1975, pp. 651-688.

2. Valera, Julio E., Seed, H. Bolton, Tsai, C.F. and Lysmer, J. (1977) "Soil-Structure Interaction Effects at the Humboldt Bay Power Plant in the Ferndale Earthquake of June 7, 1975," Journal of the Geotechnical Engineering Division, ASCE, Vol. 103, No. GT10, October, 1977.

WRITTEN CONTRIBUTION CONTRIBUTION ÉCRITE

E. Franke (F.R.G.)

A detail of the investigations for the foundation of Fig. 1 on sand in the North-Sea is presented as it may be of generel interest. Following the concept of Bjerrum (see Geotechnique 1973, p.319) the stresses beneath the shallow foundation created by cyclic wave action were simulated in the laboratory.The corresponding accumulation of excess pore pressure was determined in undrained tests with a new simple shear device shown in Fig.2; a typical result is shown in Fig. 3. In the new shear device stress controlled vertical load transmission is similar to usual triaxial tests. But different to triaxial tests the horizontal diameter of the specimen is automatically held constant during consolidation as well as during the following shear procedure, which is done by moving the top cap in horizontal direction. - In these tests it proved to be an essential problem that in sandy soil the penetration of the rubber membrane into the pore voids at the vertical surface of the specimen changes with changing excess pore water pressure Δu as shown in Fig.4. This volume change of the voids at the boundary allows for a partial drainage of the specimen and correspondingly causes a lower excess pore water pressure Δu. For calculation the safety against sliding (shown in Fig. 1) the safe determination of Δu (i.e. without drainage) is the aim of the test, deviating from triaxial tests where the effective shear parameters c' φ' are aimed and hence partial drainage may be allowed for. Therefore the described reduction of Δu caused by membrane penetration must be avoided. This can be done by placing a thin layer of liquid rubber on the membrane before fitting it to the specimen. Fig. 4 shows the effect of the preparation schematically. In Fig. 5 the great difference of the measured excess pore water pressures

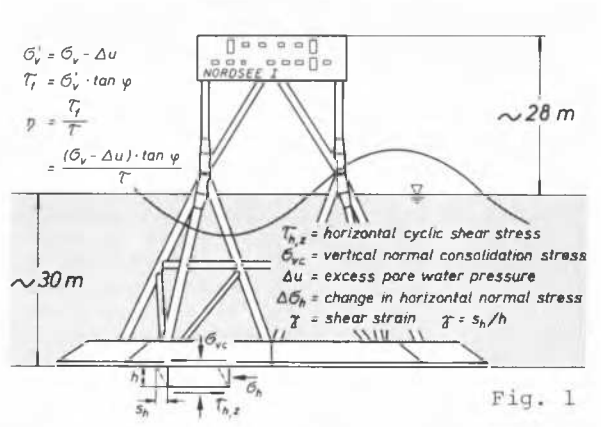

Fig. 1

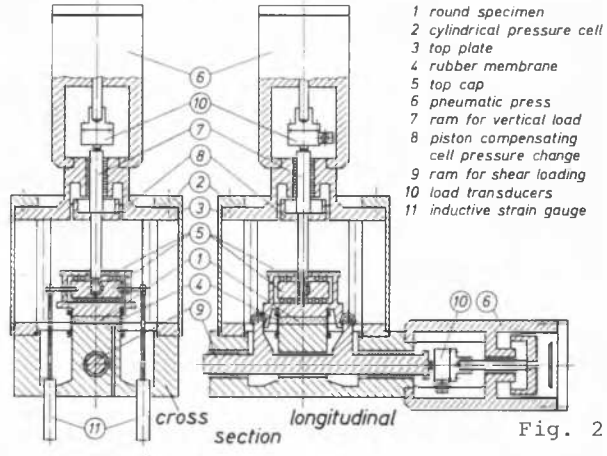

Fig. 2

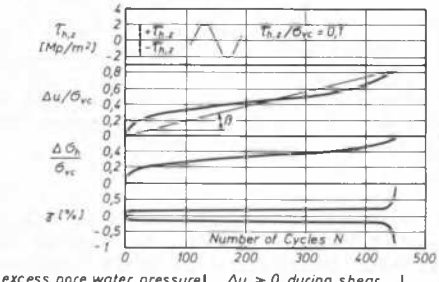

Fig. 3

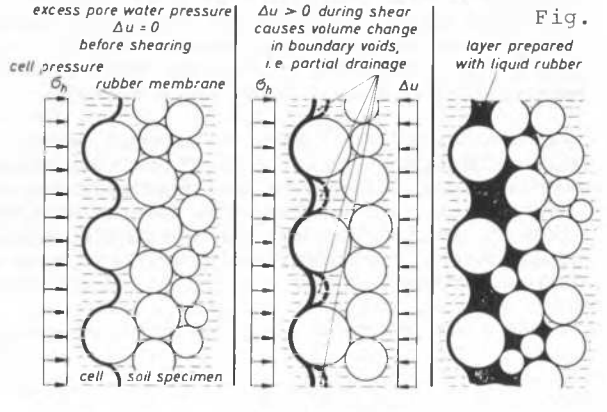

Fig. 4

Δu developing with and without using the prepared membrane can be seen. These test results were obtained by CU-triaxial tests on medium sand in the shear device of Fig.2 (because of the flat specimen not loaded to failure). For details see Kiekbusch and Schuppener,Membrane penetration, Proc. ASCE, GT

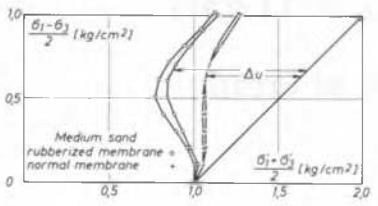

Fig. 5